IEEE Access
Multidisciplinary | Rapid Review | Open Access Journal

Received October 28, 2021, accepted December 11, 2021, date of publication December 27, 2021, date of current version January 10, 2022.

Digital Object Identifier 10.1109/ACCESS.2021.3138972

A Profit-Maximizing Security-Constrained IV-AC Optimal Power Flow Model & Global Solution

AMRO M. FARID, (Senior Member, IEEE)
Thayer School of Engineering, Dartmouth College, Hanover, NH 03755, USA
MIT Department of Mechanical Engineering, Cambridge, MA 02139, USA
e-mail: amfarid@dartmouth.edu; amfarid@mit.edu

ABSTRACT Since its first formulation in 1962, the Alternating Current Optimal Power Flow (ACOPF) problem has been one of the most important optimization problems in electric power systems. Its most common interpretation is a minimization of generation costs subject to network flows, generator capacity constraints, line capacity constraints, and bus voltage constraints. The main theoretical barrier to its solution is that the ACOPF is a non-convex optimization problem that consequently falls into the as-yet-unsolved space of NP-hard problems. To overcome this challenge, the literature has offered numerous relaxations and approximations of the ACOPF that result in computationally *suboptimal* solutions with potentially *degraded reliability*. While the impact on reliability can be addressed with active control algorithms, energy regulators have estimated that the sub-optimality costs the United States ~$6-19B per year. Furthermore, and beyond its many applications to electric power system markets and operation, the sustainable energy transition necessitates renewed attention towards the ACOPF. This paper contributes a profit-maximizing security-constrained current-voltage AC optimal power flow (IV-ACOPF) model and *globally optimal* solution algorithm. More specifically, it features a convex separable objective function that reflects a two-sided electricity market. The constraints are also separable with the exception of a set of linear network flow constraints. Collectively, the constraints enforce generator capacities, thermal line flow limits, voltage magnitudes, power factor limits, and voltage stability. The optimization program is solved using a Newton-Raphson algorithm and numerically demonstrated on the data from a transient stability test case. The theoretical and numerical results confirm the globally optimal solution.

INDEX TERMS Electric power systems engineering, optimization, optimal power flow, ACOPF, DCOPF, electricity markets.

I. INTRODUCTION

Since its first formulation in 1962 [1], the Alternating Current Optimal Power Flow (ACOPF) problem has been one of the most important optimization problems in electric power systems. Its most common interpretation is a minimization of generation costs subject to network flows, generator capacity constraints, line capacity constraints, and bus voltage constraints [2], [3]. Although a globally optimal solution to the ACOPF itself remains elusive, its most common approximation, the DCOPF (Direct Current Optimal Power Flow), has been at the heart of many wholesale deregulated ''real-time'' energy markets found at many North American Independent System Operators (ISOs) [4]–[6]. Furthermore, the DCOPF often serves as the ''sub-problem'' in mixed-integer, security-constrained, unit commitment optimization models [7]–[10] and generation and transmission planning models [11]–[14]. These, in turn, serve as the basis of wholesale ''day-ahead'' energy markets in the same ISOs. Beyond these ''economic-control'' applications, the ACOPF has also served as a reliability tool for grid operators. The generation cost objective function can also be replaced with a minimization of electric power losses or load-shedding amongst other operational objectives depending on grid conditions [2], [3].

Consequently, these many applications have motivated extensive attention towards the ACOPF. The main theoretical barrier is that the ACOPF is a non-convex optimization problem and thus falls into the as-yet-unsolved space of NP-hard problems [3]. To overcome the lack of convexity, the literature has offered numerous relaxations and approximations of the non-convex constraints including: the copper plate relaxation, the network flow relaxation,

The associate editor coordinating the review of this manuscript and approving it for publication was Ali Raza.

the Second Ordered Cone Programming (SOCP) relaxation, the Quadratic Convex (QC) relaxation, the Semi-Definite Programming relaxation (SDP), and the well-known DCOPF approximation [15]. These approaches result in computationally feasible, polynomial-time algorithms at the expense of potentially degraded reliability. In addition to the above, the literature has also offered numerous non-deterministic optimization methods including: Evolutionary Algorithms (EAs) [16]–[20], Particle Swarm Optimization (PSO) [21]–[27], Simulated Annealing (SA) [28]–[30], Artificial Neural Networks (ANN) [31]–[34], and Chaos Optimization Algorithms (COA) [35]. Despite these advances, the classification of the ACOPF in the NP-hard space has meant that a globally optimal solution remains elusive to either the detriment of system reliability or electricity costs. One author at FERC (Federal Energy Regulatory Commission) estimates that more efficient market dispatch can save the United States ~$6-19B per year [3].

Although the ACOPF problem already has an extensive history, the sustainable energy transition necessitates renewed attention. 1) First, in order to support the integration of distributed generation [36]–[39] and energy storage [40], electric power system markets are expanding beyond their traditional implementation as wholesale markets in the transmission system to retail markets in the distribution system [41]–[45] and microgrids [46]–[50]. This constitutes a dramatic proliferation of the optimal power flow problem from the nine North American independent system operators to potentially thousands of electric distribution system utilities [51]. 2) Furthermore, the radial and large-scale nature of distribution systems necessitates scalable ACOPF algorithms [36], [52]–[54]. 3) Distribution systems must also feature a prominent role for line losses, nodal voltages, and reactive power flows which disqualifies many of the typical OPF approximations [52]. 4) Fourth, the integration of variable renewable energy resources further necessitates the participation of demand-side resources in two-sided markets [36], [53], [54]. 5) Finally, as the electric power grid activates these demand–side resources, it also integrates itself with the operation of other infrastructures including water [55]–[58], transportation [59], industrial production [60], natural gas [61]–[64] and heat [65]–[68]. The non-linearity and non-convexity of the electric power network flow equations – as they are commonly stated – impedes the effective coupling of multiple infrastructure sectors. Collectively, these reasons indicate that the ACOPF problem needs an alternative formulation and not just a new solution algorithm. Furthermore, it is of immediate importance to many grid stakeholders including transmission system operators, distribution system operators, and electric utilities.

A. ORIGINAL CONTRIBUTION

The original contribution of this paper is a profit-maximizing security-constrained current-voltage AC optimal power flow (IV-ACOPF) model and globally optimal algorithm. The main novelties are as follows. 1) This ACOPF formulation has as decision variables, the real and imaginary components of the generator currents, the real and imaginary components of the line currents, and the real and imaginary components of the generator and bus voltages. Unlike other IV-ACOPF formulations, active and reactive power variables are not included to avoid non-convex feasible regions. The reliance on IV variables eliminates the non-convexities of the network flow constraints. 2) Rather than using the ''power-flow analysis'' model, a steady-state current-injection model of the physical power grid is used. As a result, generator terminal voltages are connected to exactly one other bus through a lead line. 3) A profit maximization objective function is introduced so as to create an explicit two-sided (rather than one-sided) energy market. 4) Box constraints on generator current capacities are derived from the capability curves of synchronous generators. 5) Unlike other ACOPF formulations where they are often neglected, voltage stability constraints are introduced for further reliability. 6) Finally, a power factor constraint is included as a reliability requirement enforced by many grid codes [69], [70]. This new reformulation of the ACOPF is solved via a Newton-Raphson algorithm and proven to converge to the globally optimal solution in polynomial time. The numerical results confirm a globally optimal solution for feasible loading conditions and returns an infeasible result otherwise. The paper proves that the provided IV-ACOPF formulation is a generalization of the familiar ACOPF in $PQV\theta$ variables.

B. PAPER OUTLINE

The remainder of this work is structured as follows: In Section II, a typical ACOPF formulation is introduced and some of the recent solution algorithms are presented. Section III derives the new formulation of the IV-ACOPF and proves its classification as a convex optimization program. Section IV presents the Newton-Raphson solution algorithm and proves its convergence to the globally optimal solution. Section V, then, demonstrates the IV-ACOPF formulation and solution on data from a well-known transient stability test case. Section VI discusses the novel features of this IV-ACOPF reformulation and concludes that it is a generalization of the ACOPF in $PQV\theta$ variables.Finally, Section VII concludes the work.

II. BACKGROUND

The first full formulation of the Optimal Power Flow (OPF) problem was presented by Carpentier in 1962 [1]. Since then, faster computational resources, the restructuring of electricity markets, and the proliferation of diverse (physical) energy resources on the grid have resulted in a rich volume of OPF literature spanning six decades. Surveys that look at the evolution and different approaches to solving the problem include [3], [35], [71]–[79]. Most typically, the objective function of the OPF problem is the minimization of generation costs or maximization of power grid profit. However, operators often choose other objectives including the mini-

mization of losses, the minimization of load-shedding, among other possibilities.

Equations 1-7 collectively depict a typical formulation of the ACOPF problem using '$PQV\theta$' decision variables.

$$min \quad \sum_{g\in\mathcal{G}}\left(\alpha_{Rg}P_g^2+\beta_{Rg}P_g+\gamma_{Rg}\right) - \sum_{d\in\mathcal{D}}\left(\alpha_{Rd}P_d^2+\beta_{Rd}P_d+\gamma_{Rd}\right) \tag{1}$$

$$s.t. \sum_{g\in\mathcal{G}}A_{gd}P_g - P_d = |V_d|\sum_{d'\in\mathcal{D}}|V_{d'}|\left(g_{dd'}\cos(\theta_{dd'})+b_{dd'}\sin(\theta_{dd'})\right) \quad \forall d\in\mathcal{D} \tag{2}$$

$$\sum_{g\in\mathcal{G}}A_{gd}Q_g - Q_d = |V_d|\sum_{d'\in\mathcal{D}}|V_{d'}|\left(g_{dd'}\sin(\theta_{dd'})-b_{dd'}\cos(\theta_{dd'})\right) \quad \forall d\in\mathcal{D} \tag{3}$$

$$\theta_{v1}=0 \tag{4}$$

$$P_g^{min}\le P_g\le P_g^{max} \quad \forall g\in\mathcal{G} \tag{5}$$

$$Q_g^{min}\le Q_g\le Q_g^{max} \quad \forall g\in\mathcal{G} \tag{6}$$

$$0\le P_\ell\le P_\ell^{max} \quad \forall \ell\in\mathcal{L} \tag{7}$$

$$|V_d|^{min}\le|V_d|\le|V_d|^{max} \quad \forall d\in\mathcal{D} \tag{8}$$

To elaborate, this formulation uses the ''power flow analysis'' model of an electric power system. It includes a set of demand buses $\mathcal{D}$ with its associated vector of voltage phasors $V_D=|V_D|\angle\theta_{VD}$ as decision variables and complex power withdrawals $S_D=P_D+jQ_D$ as imposed exogeneous constants. Consequently, this typical formulation assumes *inelastic demand* for electric power. The power system model also includes a set of generators $\mathcal{G}$ with its associated vector of complex power injections $S_G=P_G+jQ_G$ as decision variables. The power system model also includes power lines $\mathcal{L}$. These have their associated vector of complex power flows $S_\mathcal{L}=P_L+jQ_L$ as decision variables. The model relies on the formulation of a bus admittance matrix $Y=G+jB$ such that the subscript notation of the scalars $g_{dd'}$ and $b_{dd'}$ indicate the (d,d') element of the G and B matrices respectively. Similarly, the notation $\theta_{dd'}$ is the voltage phase angle difference between demand buses d and d'. A_{GD} is the generator to demand bus incidence matrix indicating a value of 1 when generator g is connected to bus d. Finally, α_{Rg}, β_{Rg}, and γ_{Rg} are the quadratic, linear, and fixed cost terms of the active power injections by each generator $g\in\mathcal{G}$ and α_{Rd}, β_{Rd}, and γ_{Rd} are the quadratic, linear, and fixed terms of the active power withdrawals at each demand bus $d\in\mathcal{D}$.

As a whole, this formulation of the ACOPF maximizes profit subject to physical reliability constraints. Equation 1 is the (negative) profit objective function (to be minimized) that is composed of a convex quadratic cost function of the active power generated and a convex quadratic revenue function of the active power consumed. Note that because the vector of active power demands P_D is an *exogeneous constant*, the revenue terms in this *two-sided market formulation* are very commonly dropped to produce an *equivalent one-sided market formulation* in which the objective function is written as a simple minimization of generation costs:

$$min \sum_{g\in\mathcal{G}}\alpha_{Rg}P_g^2+\beta_{Rg}P_g+\gamma_{Rg} \tag{9}$$

Equation 2 is the network flow constraint for active power, Equation 3 is the network flow constraint for reactive power, Equation 4 indicates the reference angle of the network, Equation 5 is the active power capacity constraint, Equation 6 is the reactive power capacity constraint, Equation 8 is the voltage magnitude constraint at a bus, and Equation 7 is the line flow limit constraint. Also note that Equations 2 and 3 collectively make the ACOPF problem non-linear and non-convex. In order to overcome the problems caused by the non-linearity and non-convexity of these constraints, an extensive literature has emerged that proposes numerous relaxations, approximations, and solution algorithms.

Perhaps the most commonly deployed approximation, especially in electric energy markets, is the so-called ''DCOPF'' problem [3]. It is obtained by setting all voltage magnitudes to unity, eliminating lines losses (i.e. G = 0), and linearizing the power flow equations via a small-angle approximation [80]. Despite its broad adoption, the DCOPF approximation cannot be used universally; including in distribution systems where line losses are non-negligible [52]. Furthermore, a DCOPF solution may not satisfy the original nonlinear power flow equations. Under such circumstances, an operator might tweak the DCOPF solution through a subsequent solution of the power flow analysis equations. The DCOPF can also over-constrain the solution space; potentially generating an infeasible solution even when the ACOPF remains feasible. Finally, there is no guarantee that the obtained DCOPF solution is either locally or globally optimal and estimation of the distance from global optimality remains a topic of research [81].

Consequently, much of the recent ACOPF literature has sought to use reformulations that involve Convex Relaxations (CR). In such works, non-convex constraints are loosened to form a larger, but more importantly, convex feasible region. The main advantage of such an approach is that if the new CR algorithm returns an optimal solution within the original non-convex region, then it has also solved the original (non-convex) problem as well. Furthermore, if the new CR algorithm returns an infeasible solution, then the original (non-convex) problem was as well. Several CRs have appeared in the recent ACOPF literature. One of the most promising relaxations to the ACOPF problem, the Second Order Cone Programming (SOCP) was proposed for radial networks by Jabr in 2006 [82]. Since then, the semi-definite programming (SDP) relaxation has garnered a lot of attention for its robustness and performance in the literature

[83]–[85]. In particular, Lavaie and Low have shown topological conditions where the SDP relaxation demonstrates a zero duality gap and, therefore, returns a globally optimal solution [86]. Finally, the Quadratic Convex (QC) relaxation has been shown to be promising, producing results that are also robust and reliable [87]. It has also been shown that certain types of network topologies can guarantee a globally optimal solution [88], [89]. For radial networks, some of the aforementioned relaxations have proved to be equivalent, with a bijective map between their feasible set [90].

Finally, a relatively small portion of the ACOPF literature abandons the active power (P), reactive power (Q), voltage magnitude ($|V|$), and voltage phase angle (θ) decision variables in favor of novel combinations of not just P and Q but also the voltage (V) and current phasors ($\mathcal{I}$) in rectangular coordinates. A rectangular IV-PQ formulation has been proposed and has demonstrated good computational performance despite a lack of convexity [75], [91], [92]. A power-current hybrid formulation has also been proposed with similar effect [93]. The premise of these works is the assertion that if the non-convexity in the network wide flow constraint can be isolated to the buses and made separable, the formulation becomes more amenable to a relaxation [75], [91]. The following section proceeds within this general category of IV-ACOPF formulations with several novel additions.

III. IV-ACOPF FORMULATION

This section derives an IV-ACOPF formulation in rectangular coordinates using a current-injection model [94] equivalent to the one use in transient stability analysis studies after steady-state conditions have been achieved. As is elaborated in Section VI, this steady-state current injection model provides many advantages; most notably the ability to separate all power system nodes into two distinct groups; generator terminals and demand-buses. In addition to the constraints found in the traditional formulation of the optimal power flow problem, three additional physical phenomena are included in this formulation. First, a current injection model rather than power flow analysis model is used. Therefore, each generator receives its associated lead line in the network flow [94], [95]. Second, voltage stability imposes a constraint on the difference in voltage phase angle between two buses [94], [95]. Some $PQV\theta$ formulations have introduced voltage stability constraints [96]–[99], but an extensive search has yet to reveal their introduction into an IV-ACOPF. Lastly, the net power injection into a given bus is placed within minimum and maximum power factor limits to reflect IEEE operating standards [95].

The elaboration of the IV-ACOPF formulation proceeds as follows. Sec. III-A contrasts the current injection model to the power flow analysis model. Sec. III-B then derives the associated network flow equations from first engineering principles. Next, Sec. III-C derives the objective function from first economic principles. The section then follows the ACOPF formulation described in Section II with Sec. III-D, III-E, III-F and III-G describing the reference voltage, generator capacity, thermal line flow, voltage magnitude constraints respectively. The power factor and voltage stability constraints are then added as new constraints in Sections III-H and III-I respectively. Finally, in order to create a convex feasible region, a high quality relaxation of the voltage magnitude lower bound is introduced in Sec. III-J. Section IV later proves that the introduction of such a relaxation does not impede a solution to a global optimum.

A. THE STEADY-STATE CURRENT INJECTION MODEL

The current injection model is a well established power systems engineering model that is used to study the ''transient (angle) stability'' of a power system in response to various disruptions [94], [95]. The power flow analysis model used in the traditional ($PQV\theta$) ACOPF problem above corresponds with the green buses and blue lines in Fig. 1. Generators and loads appear as power injections directly into or out of these buses. The current injection model, instead, treats each generator as a voltage source attached to a lead line. For transient stability analyses, usually in the 0.1-10Hz timescale, each of these generators is given a differential equation called a ''swing equation''. Then the system-wide stability is assessed either by numerical simulation in response to a perturbation or directly by analytical methods. As the optimal power flow problem is typically run every five minutes, one can reasonably assume that swing equation dynamics have reached steady state and can be subsequently neglected for the remainder of the paper.

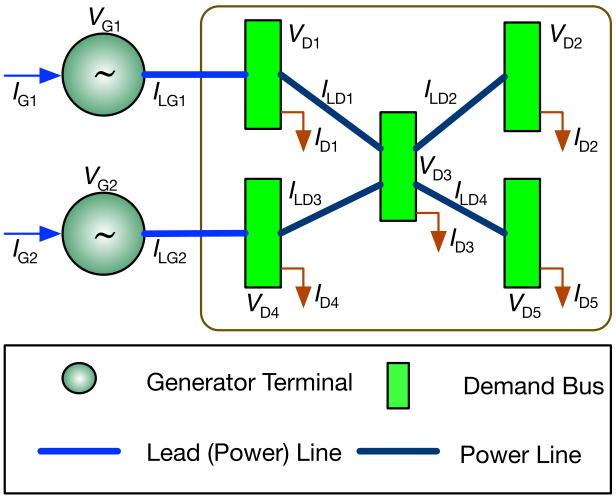

FIGURE 1. The Power Flow Analysis vs the Steady State Current Injection Model. The power flow analysis model includes the green buses, their associated power demands, and the blue power lines. Generators are modeled as power injections directly into some of the buses. The current injection model replaces these power injections with a lead line attached to a generator represented as a voltage source with its associated current injection [94], [95].

As shown in Figure 1, this steady-state current injection model has a set of demand buses $\mathcal{D}$ with its associated vector of voltages $V_D = V_{DR} + jV_{DI}$ and current withdrawals $\mathcal{I}_D = \mathcal{I}_{DR} + j\mathcal{I}_{DI}$ which are taken as exogeneous data inputs.

It also has a set of generators $\mathcal{G}$ with its associated vector of voltages $V_G = V_{GR} + jV_{GI}$ and current injections $\mathcal{I}_G = \mathcal{I}_{GR} + j\mathcal{I}_{GI}$. The power lines $\mathcal{L} = \mathcal{L}_G \cup \mathcal{L}_D$ are partitioned into lead lines $\mathcal{L}_G$ and the power lines $\mathcal{L}_D$ of the original power flow analysis network. These have their associated vector of currents $\mathcal{I}_\mathcal{L} = \mathcal{I}_{\mathcal{L}R} + j\mathcal{I}_{\mathcal{L}I} = [\mathcal{I}_{\mathcal{L}G}; \mathcal{I}_{\mathcal{L}D}]$. The constants $N_\mathcal{G}$, $N_\mathcal{D}$ and $N_\mathcal{L} = N_{\mathcal{L}\mathcal{G}} + N_{\mathcal{L}\mathcal{D}}$ are also introduced to reflect the number of generators, demand buses, and power lines. The remainder of this section formulates the IV-ACOPF on the basis of this current injection model under steady state conditions. Equations 1-7 are discussed in sequence. As the discussion of the objective function depends on the network flow constraints, the latter are derived first.

B. NETWORK FLOW CONSTRAINTS

Because the network flow equations in Equations 2 and 3 apply to the power flow analysis model and are expressed in PQ variables, they are not a suitable starting point for this derivation. Instead, the network flow equations are re-derived from the first principles of Kirchoff's Current Law and Ohm's law. For the current injection model shown in Fig. 1, Kirchoff's Current Law in rectangular coordinates gives:

$$\begin{bmatrix} \mathcal{I}_{GR} \\ -\mathcal{I}_{DR} \end{bmatrix} = \begin{bmatrix} A_G^T \\ A_D^T \end{bmatrix} \mathcal{I}_{LR} \tag{10}$$

$$\begin{bmatrix} \mathcal{I}_{GI} \\ -\mathcal{I}_{DI} \end{bmatrix} = \begin{bmatrix} A_G^T \\ A_D^T \end{bmatrix} \mathcal{I}_{LI} \tag{11}$$

where $\mathcal{I}_G$ and $\mathcal{I}_D$ have opposite sign convention according to Fig. 1, and where A_G is the line to generator incidence matrix,

$$A_G(l, g) = \begin{cases} 1 & \text{if line } l \text{ originates at generator } g \\ -1 & \text{if line } l \text{ terminates at generator } g \\ 0 & \text{otherwise} \end{cases} \tag{12}$$

and where A_D is the line to bus incidence matrix.

$$A_D(l, d) = \begin{cases} 1 & \text{if line } l \text{ originates at demand bus } d \\ -1 & \text{if line } l \text{ terminates at demand bus } d \\ 0 & \text{otherwise} \end{cases} \tag{13}$$

So as to distinguish between lead lines and power lines shown in Figure 1, it is also useful to partition these incidence matrices: $A_G = [A_{GG}; 0]$ and $A_D = [A_{DG}; A_{DD}]$ and recognize that $A_{DG} = -A_{GD}$ (as defined previously). Then, Ohm's Law in complex matrix form gives:

$$\mathcal{I}_L = Y_L(A_G V_G + A_D V_D) \tag{14}$$

$$\mathcal{I}_L = Y_L[A_G \;\; A_D] \begin{bmatrix} V_G \\ V_D \end{bmatrix} \tag{15}$$

where $Y_L = G_L + jB_L$ is constructed from the vector of admittances of the lead lines $\mathcal{Y}_G$ and the vector of admittances of the power lines $\mathcal{Y}_D$. $Y_L = diag(\mathcal{Y}_L) = diag([\mathcal{Y}_{LG}; \mathcal{Y}_{LD}])$. Switching to rectangular components gives:

$$\mathcal{I}_{LR} = G_L[A_G \;\; A_D] \begin{bmatrix} V_{GR} \\ V_{DR} \end{bmatrix} - B_L[A_G \;\; A_D] \begin{bmatrix} V_{GI} \\ V_{DI} \end{bmatrix} \tag{16}$$

$$\mathcal{I}_{LI} = B_L[A_G \;\; A_D] \begin{bmatrix} V_{GR} \\ V_{DR} \end{bmatrix} + G_L[A_G \;\; A_D] \begin{bmatrix} V_{GI} \\ V_{DI} \end{bmatrix} \tag{17}$$

which simplifies straightforwardly by evaluating the matrix products:

$$\begin{bmatrix} A_G^T \\ A_D^T \end{bmatrix} \mathcal{I}_{LR} = G \begin{bmatrix} V_{GR} \\ V_{DR} \end{bmatrix} - B \begin{bmatrix} V_{GI} \\ V_{DI} \end{bmatrix} \tag{18}$$

$$\begin{bmatrix} A_G^T \\ A_D^T \end{bmatrix} \mathcal{I}_{LI} = B \begin{bmatrix} V_{GR} \\ V_{DR} \end{bmatrix} + G \begin{bmatrix} V_{GI} \\ V_{DI} \end{bmatrix} \tag{19}$$

where G and B are the nodal conductance and susceptance matrices respectively.

$$G = [A_G \;\; A_D]^T G_L [A_G \;\; A_D] \tag{20}$$

$$B = [A_G \;\; A_D]^T B_L [A_G \;\; A_D] \tag{21}$$

Equations 10, 11, 18 and 19 constitute a steady-state current-injection model and are incorporated into the new IV-ACOPF formulation.

C. OBJECTIVE FUNCTION

Returning back to the objective function of the ACOPF, the translation of the quadratic function in Equation 1 to voltage and current variables requires especially careful attention. Consider a naive change of variable of the active power generated P_g:

$$\begin{aligned} P_g &= \Re\{V_g \mathcal{I}_g^*\} \\ &= \Re\{(V_{Rg} + jV_{Ig})(\mathcal{I}_{Rg} + j\mathcal{I}_{Rg})^*\} \\ &= \Re\{(V_{Rg} + jV_{Ig})(\mathcal{I}_{Rg} - j\mathcal{I}_{Ig})\} \\ P_g &= V_{Rg}\mathcal{I}_{Rg} + V_{Ig}\mathcal{I}_{Ig} \end{aligned} \tag{22}$$

The Hessian of the function in Eq. 22 has eigenvalues $\lambda_e = \{-1, -1, 1, 1\}$ and therefore has indefinite convexity. A similar conclusion is straightforwardly made for a reactive power function of voltage and current. Furthermore, convex functions that are composed of functions of indefinite convexity also have indefinite convexity [100], [101]. This fact serves as a strong caution against any ACOPF reformulation that combines PQ variables with IV variables. Instead, this work develops a formulation on *exclusively* IV variables as shown in the remainder of this work.

The derivation of the objective function $\mathcal{J}$ begins with the well-held economic principle that (in the absence of other constraints) market equilibrium is achieved when the sum of all of Marginal Revenues (MR) and Marginal Costs (MC) equals zero.

$$\nabla J = \sum_{g \in \mathcal{G}} \text{MC}_g - \sum_d \text{MR}_d \tag{23}$$

The earliest works in power system economics; including the first formulations of the economic dispatch, DCOPF, and ACOPF assumed that demand was inflexible and constant in a single time step [102]. Therefore, revenue/utility terms from the demand-side were assumed as constants and were abstracted away in favor of one-sided cost-minimization markets. While this work retains the inflexible and constant demand assumption, the revenue terms are explicitly re-introduced so as to create an explicitly two-sided market with inelastic demand.

Next, each generator is given a linear marginal cost curve and each demand-bus is given a linear marginal revenue curve.

$$\nabla J = \begin{bmatrix} \partial J/\partial P \\ \partial J/\partial Q \end{bmatrix} = \sum_{g\in\mathcal{G}} \left(\alpha_g \cdot S_g + \beta_g\right) - \sum_{d\in\mathcal{D}} \left(\alpha_d \cdot S_d + \beta_d\right) \tag{24}$$

where $(\cdot)$ is the element-wise Hadamard product [103] and where $\alpha_g = [\alpha_{Rg}; \alpha_{Ig}]$, $\alpha_d = [\alpha_{Rd}; \alpha_{Id}]$, $\beta_g = [\beta_{Rg}; \beta_{Ig}]$, $\beta_d = [\beta_{Rd}; \beta_{Id}]$ are real two-dimensional vectors. Unlike the objective function shown in Eq. 1, this work assumes, for generality, that both active and reactive power generation can incur cost and that active and reactive power consumption can generate revenue. In other words, this IV-ACOPF treats both active and reactive power as monetized and exchanged products. Furthermore, this work retains the common assumption of increasing marginal costs and therefore assumes that both components of α_g are positive. Similarly, this work retains the common assumption of decreasing marginal revenues and therefore assumes that both the components of α_d are negative. Nevertheless, taking the gradient of Eq. 1 immediately results in Eq. 24 with $\alpha_{Ig} = \alpha_{Id} = \beta_{Ig} = \beta_{Id} = 0 \quad \forall g \in \mathcal{G}, d \in \mathcal{D}$.

Several algebraic manipulations are now required in order to convert the non-convex Eq. 24 into an equivalent equation written in IV variables that is convex. Substituting the complex power definition $S = V \star \mathcal{I}^*$ yields:

$$\nabla J = \sum_{g\in\mathcal{G}} \left(\alpha_g \cdot V_g \star \mathcal{I}_g^* + \beta_g\right) - \sum_{d\in\mathcal{D}} \left(\alpha_d \cdot V_d \star \mathcal{I}_d^* + \beta_d\right) \tag{25}$$

Here the $\star$ notation is introduced to emphasize the multiplication of complex numbers so as to distinguish between matrix multiplication and the element-wise Hadamard product. $[a_R; ja_I] \star [b_R; jb_I] = [a_R b_R + a_I b_I; a_R b_I + a_I b_R]$. In scalar form, Kirchhoff's current balance at each demand-bus d follows from Eq. 10 and 11:

$$-\mathcal{I}_d = \sum_{l\in\mathcal{L}} A_D(l,d)\mathcal{I}_l \tag{26}$$

$$-\mathcal{I}_d = \sum_{l_g\in\mathcal{L}} A_{DG}(l_g,d)\mathcal{I}_{l_g} + \sum_{l_d\in\mathcal{L}} A_{DD}(l_d,d)\mathcal{I}_{l_d} \tag{27}$$

Returning to the linear revenue term $(\alpha_d \cdot V_d I_d^*)$ in Eq. 25, it is then expressed as a linear combination of revenue components originating from each connected line and lead line. More specifically, complex power coming over a lead line l_g will have an associated retail rate of $\rho_d + \alpha_g$ while a regular power line will have an associated retail rate of ρ_d.

$$\alpha_d \cdot V_d I_d^* = -(\rho_d + \alpha_g)\cdot V_d \star \sum_{l_g\in\mathcal{L}_G} A_{DG}(l_g,d)\mathcal{I}_{l_g}^* - \rho_d \cdot V_d \star \sum_{l_d\in\mathcal{L}_D} A_{DD}(l_d,d)\mathcal{I}_{l_d}^* \tag{28}$$

where both components of the effective retail rate ρ_d are assumed to be negative to maintain the assumption of diminishing marginal revenues. Recognizing that there is only one lead line l_g for each generator g, and substituting in Eq. 28, Eq. 25 then simplifies to:

$$\nabla J = \sum_{g\in\mathcal{G}} \left(\alpha_g \cdot \left(V_g + \sum_{d\in\mathcal{D}} A_{DG}(g,d)V_d\right) \star I_g^* + \beta_g\right) - \sum_{d\in\mathcal{D}} \left(\rho_d \cdot V_d \star I_d^* + \beta_d\right) \tag{29}$$

And then applying Ohm's law yields:

$$\nabla J = \sum_{g\in\mathcal{G}} \left(\alpha_g \cdot Z_g \star I_g \star I_g^* + \beta_g\right) - \sum_{d\in\mathcal{D}} \left(\rho_d \cdot V_d \star I_d^* + \beta_d\right) \tag{30}$$

or simply:

$$\nabla J = \sum_{g\in\mathcal{G}} \left(\alpha_g \cdot S_{\mathcal{L}g} + \beta_g\right) - \sum_{d\in\mathcal{D}} \left(\rho_d \cdot S_d + \beta_d\right) \tag{31}$$

where $S_{\mathcal{L}g}$ is the complex power lost in the lead line between a generator and a demand-bus. It must not be confused with the complex power S_g injected by generator g. Furthermore, it is worth noting that Eq. 30 is a convex function of I_g and V_d whereas Eq. 24 is not.

The (negative) profit objective function (to be minimized) is then derived as the sum of the integral of each of the components of the gradient.

$$\mathcal{J} = \int \frac{\partial J}{\partial P_{\mathcal{L}G}} dP_{\mathcal{L}G} + \int \frac{\partial J}{\partial Q_{\mathcal{L}G}} dQ_{\mathcal{L}G} + \int \frac{\partial J}{\partial P_D} dP_D + \int \frac{\partial J}{\partial Q_D} dQ_D \tag{32}$$

which evaluates to:

$$\begin{aligned}\mathcal{J} = &\sum_{g\in\mathcal{G}} \left(\alpha_{Zg}(\mathcal{I}_{Rg}^2 + \mathcal{I}_{Ig}^2)^2 + \beta_{Zg}(\mathcal{I}_{Rg}^2 + \mathcal{I}_{Ig}^2) + \gamma_{Rg} + \gamma_{Ig}\right) \\ &+ \sum_{d\in\mathcal{D}} \left(\bar{\rho}_{Rd}(V_{Rd}I_{Rd} + V_{Id}I_{Id})^2 - \beta_{Rd}(V_{Rd}I_{Rd} + V_{Id}I_{Id}) + \bar{\gamma}_{Rd}\right) \\ &+ \left(\bar{\rho}_{Id}(-V_{Rd}I_{Id} + V_{Id}I_{Rd})^2 - \beta_{Id}(-V_{Rd}I_{Id} + V_{Id}I_{Rd}) + \bar{\gamma}_{Id}\right)\end{aligned} \tag{33}$$

where $\alpha_{Zg} = (\alpha_{Rg}R_g^2 + \alpha_{Ig}X_g^2)/2$, and $\beta_{Zg} = (\beta_{Rg}R_g + \beta_{Ig}X_g)$. Also, the notation $\bar{\rho}_d = -\rho_d/2$, and $\bar{\gamma}_d = -\gamma_d$ is introduced so as to use positive leading coefficients exclusively. The constants vectors γ_g, γ_{Rd}, and γ_{Id} are introduced to account for the generator fixed costs and demand-bus fixed revenues. Notice that Eq. 33 is a *generalization* of Eq. 1 that accounts

for the cost of reactive power generation and that explicitly includes the revenues from active and reactive power consumption at the demand buses.

Consequently, this objective function implies several locational marginal quantities.

$$\partial J/\partial P_g = \alpha_{Rg} R_g^2 (\mathcal{I}_{R_g}^2 + \mathcal{I}_{I_g}^2) + \beta_{Rg} R_g \quad (34)$$

$$\partial J/\partial Q_g = \alpha_{Ig} X_g^2 (\mathcal{I}_{R_g}^2 + \mathcal{I}_{I_g}^2) + \beta_{Ig} X_g \quad (35)$$

$$\partial J/\partial P_d = \bar{\rho}_{Rd} P_d - \beta_{R_d} \quad (36)$$

$$\partial J/\partial Q_d = \bar{\rho}_{Id} Q_d - \beta_{I_d} \quad (37)$$

These marginal revenue and marginal cost terms tie into the extensive literature on locational marginal prices [104]–[107] and facilitate the use of this IV-ACOPF formulation in electricity market designs despite the novel use of IV variables.

In all, the derived objective function is separable with respect to generator lead lines and demand buses. Furthermore, it is quartic in the lead line currents and quadratic in the demand bus voltages. The work assumes exogenously fixed demand-bus current withdrawals $\mathcal{I}_D$. Although this choice of exogenous data is different from the traditional ACOPF, this data is readily available to grid operators. Furthermore, this choice of exogenous data does maintain the demand-bus voltages as decision variables.

D. REFERENCE VOLTAGE CONSTRAINT

The reference voltage constraint in Equation 4 translates straightforwardly into rectangular components.

$$V_{I_{ref}} = 0 \quad (38)$$

E. GENERATOR CAPACITY CONSTRAINTS

The conversion of the generator capacity "box" constraints in Equations 5 and 6 also requires careful attention. Despite their widespread use, it is important to recognize that there is no physics-based phenomenon that results in box constraints on active and reactive power. Instead, Carpentier's original 1962 paper chose to 1.) assume that all power plants use synchronous generators as electrical machines, and 2.) approximate a synchronous generator's capability curve with a PQ box [1]. The first assumption is entirely appropriate to the reality of predominantly thermo-electric generation in 1962, but is not necessarily valid in the present sustainable energy transition. For Carpentier's second choice, Fig. 2b shows the actual, highly-curved, shape of a synchronous generator's capability curve [108] – which is in turn derived from a synchronous generator's equivalent circuit and phasor diagram [108] (in Fig 2a). The active power upper bound originates from the circular constraint caused by the maximum stator current I_a. Meanwhile, the reactive power upper bound originates from the circular constraint caused by the maximum rotor current (which in turn is proportional to the voltage E_a). The active power lower bound is not an electrical phenomena. Instead, it represents the minimum safe operating level for a combustion-driven process (e.g. boiler or gas turbine) [109]. Fourth, the reactive power lower bound

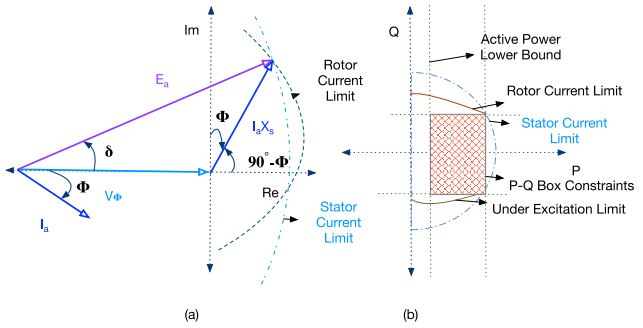

FIGURE 2. (a.) a synchronous generator's phasor diagram and the associated limits on the voltage magnitudes of E_a and I_aX_S. (b.) a synchronous generator's actual capability curve and box constraint approximation. [1], [108].

originates from rotating the maximum stator current phasor into the fourth quadrant of the complex plane to a limit of under excitation. Finally, the PQ generator capability curve is simply a synchronous generator's (voltage) phasor diagram with a 90° rotation and a *constant* conversion factor of V_ϕ/X_S where V_ϕ is the generator's one-line equivalent terminal voltage and X_S is the synchronous effective 1-line reactance of the generator [108].

In translating the generator capacity constraints to an IV formulation, this work recognizes the practical compromise between 1.) the physical modeling of the underlying complexity of generator characteristics, 2.) the socio-economic design of an *equitable* electricity market that frames all generators within the same set of applicable constraints, and 3.) the mathematical tractability of convex vs non-convex feasible regions. Therefore, it reconfirms Carpentier's box constraints with a constant V_ϕ conversion factor from active and reactive power to generator output current.

$$\mathcal{I}_{RG}^{min} \leq \mathcal{I}_{RG} \leq \mathcal{I}_{RG}^{max} \quad (39)$$

$$\mathcal{I}_{IG}^{min} \leq \mathcal{I}_{IG} \leq \mathcal{I}_{IG}^{max} \quad (40)$$

where $\mathcal{I}_{RG}^{min} = P_G^{min}/V_\phi$, $\mathcal{I}_{RG}^{max} = P_G^{max}/V_\phi$, $\mathcal{I}_{IG}^{min} = Q_G^{min}/V_\phi$, and $\mathcal{I}_{IG}^{max} = P_G^{max}/V_\phi$. Again, because the conversion from a generator's phasor diagram to its capability curve is simply a multiplication by a constant factor, the backward conversion from PQ coordinates in VA units to complex current coordinates is a division by the same factor. An added advantage of Eq. 39 and 40 is that they can be straightforwardly derived from existing ACOPF datasets; be they real or hypothetical test cases.

F. THERMAL LINE FLOW CONSTRAINTS

Next, the thermal line flow constraints in Equation 7 must be expressed in terms of complex voltages and currents.

$$0 \leq \left([A_G \;\; A_D]\begin{bmatrix} V_{GR} \\ V_{DR} \end{bmatrix}\right)\mathcal{I}_L^* \leq \left([A_G \;\; A_D]\begin{bmatrix} V_{GR} \\ V_{DR} \end{bmatrix}\right)\overline{\mathcal{I}_L^*} \quad (41)$$

Given the vector of power line impedances Z_L, substituting Ohm's law from Eq. 15 into Equation 41

and simplifying yields:

$$0 \leq \mathcal{I}_{LR}^2 + \mathcal{I}_{LI}^2 \leq |\overline{I_L}|^2 \tag{42}$$

where $()^2$ is calculated on an element by element basis.

G. VOLTAGE MAGNITUDE CONSTRAINTS

Next, the separable voltage magnitude constraint in Equation 8 is rewritten in rectangular coordinates and then squared

$$\underline{|V_D|}^2 \leq V_{DR}^2 + V_{DI}^2 \leq |\overline{V_D}|^2 \tag{43}$$

Note that the lower bound on this constraint also introduces a non-convex feasible region; a subject which is given further attention in Section III-J. The generator voltage terminals also have a separable constraint,

$$V_{GR}^2 + V_{GI}^2 \leq |\overline{V_G}|^2 \tag{44}$$

Note that a lower bound is not required because, the generator voltage magnitude will always be greater than the bus voltage magnitude of the corresponding bus because of the positive flow of generated current.

H. POWER FACTOR CONSTRAINT

The first of two constraints that must be added to the ACOPF formulation is a bounded power factor. While the power factor at each demand-bus is known in the traditional ACOPF, the switch to an IV formulation means that it no longer is. NERC and other grid operators bound the power factor of power injections at a bus to between 0.95 and 1.00 [69], [70].

$$0.95 \cdot \mathbb{1}^{N_D} \leq \frac{P_D}{S_D} \leq \mathbb{1}^{N_D} \tag{45}$$

where $\mathbb{1}^{N_D}$ is a vector of ones of length N_D, and the division $()/()$ is element-wise. Using the definition of active and complex power, Eq. 45 becomes:

$$0.95 \cdot \mathbb{1}^{N_B} \leq \cos(\theta_{VD} - \theta_{ID}) \leq \mathbb{1}^{N_D} \tag{46}$$

where again θ_{VD} is the demand bus voltage phase angles and the current withdrawal phase angles $\theta_{ID} = \tan^{-1}(\mathcal{I}_{DI}/\mathcal{I}_{DR})$. Switching from a constraint on $\cos(\theta_{VD} - \theta_{ID})$ to $\tan(\theta_{VD})$ and then converting to rectangular coordinates results in two sets of separable constraints:

$$V_{DI} - V_{DR}\tan(\theta_{VD}^{max}) \leq 0 \tag{47}$$
$$0 \leq V_{DI} - V_{DR}\tan(\theta_{VD}^{min}) \tag{48}$$

where $\theta_{VD}^{max} = 18.19^\circ + \theta_{ID}$ and $\theta_{VD}^{min} = -18.19^\circ + \theta_{ID}$. Although the choice of reference bus is entirely arbitrary, the common practice is to choose a bus connected to a generator (via a lead line). In such a case, the reference bus often has among the larger voltage phase angles in the power system. Furthermore, if the reference bus is chosen to have the largest voltage phase angle, then $\theta_{VD}^{max} = 0$.

I. VOLTAGE STABILITY CONSTRAINT

In addition to the above, the power system lines and generator's lead line must maintain voltage stability; expressed as a voltage angle difference inequality constraint.

$$\begin{bmatrix} \Delta\theta_{VG}^{min} \\ \Delta\theta_{VD}^{min} \end{bmatrix} \leq \left([A_G \;\; A_D] \begin{bmatrix} \theta_{VG} \\ \theta_{VD} \end{bmatrix} \right) \leq \begin{bmatrix} \Delta\theta_{VG}^{max} \\ \Delta\theta_{VD}^{max} \end{bmatrix} \tag{49}$$

where $\Delta\theta_{VD}^{min}$ and $\Delta\theta_{VD}^{max}$ represent vectors of the minimum and maximum voltage phasor angle differences between connected demand buses in the network, and $[\theta_{VG}; \theta_{VD}]$ is the vector of nodal voltage angles.

In most practical applications, $\Delta\theta_{VD}^{min}$, $\Delta\theta_{VD}^{max}$, $\Delta\theta_{VGD}^{min}$, and $\Delta\theta_{VGD}^{max}$ are small in magnitude. Next, Equation 49 can be rewritten as a constraint on the current phase angle using Ohm's law. Given an arbitrary power line l with a voltage difference ΔV_l across it, the current phasor is:

$$\mathcal{I}_l = \frac{|\Delta V_l| e^{i(\Delta\theta_{vl})}}{|z_l| e^{i(\theta_{zl})}} = \frac{|\Delta V_l|}{|z_l|} e^{i(\Delta\theta_{vl} - \theta_{zl})} \qquad \forall l \in \mathcal{L} \tag{50}$$

Consequently, the vector of current phase angles is:

$$\theta_L = [A_G \;\; A_D] \begin{bmatrix} \theta_{VG} \\ \theta_{VD} \end{bmatrix} - \theta_{ZL} \tag{51}$$

Substituting Eq. 51 into Eq. 49.

$$\theta_L^{min} \leq \theta_L \leq \theta_L^{max} \tag{52}$$

where $\theta_L^{min} = \Delta\theta_{BV}^{min} - \theta_{ZL}$ and $\theta_L^{max} = \Delta\theta_{VGD}^{max} - \theta_{ZL}$. Equation 52 is then rewritten in rectangular coordinates to yield two sets of separable constraints.

$$I_{LI} - I_{LR}\tan(\theta_L^{max}) \leq 0 \tag{53}$$
$$0 \leq I_{LI} - I_{LR}\tan(\theta_L^{min}) \tag{54}$$

where tan() is calculated on an element by element basis.

J. RELAXING THE NON-CONVEX LOWER BOUND CONSTRAINTS ON VOLTAGE MAGNITUDES

A careful inspection of Equation 43 reveals that the lower bounds on the demand bus voltage magnitudes create a non-convex feasible region. Neglecting the network flow constraints, and taking advantage of the separable nature of the remainder of the IV-ACOPF formulation, a graphical approach serves to develop intuition. Figure 3 shows the feasible region of the real and and imaginary components of the voltage at an arbitrarily chosen demand bus $V_d = V_{Rd} + jV_{Id}$. The "halo"-shaped region in dark grey is caused by the upper and lower bounds on the voltage magnitude in Eq. 43 and corresponds to the original ACOPF problem in Section II. The forrest green region $\mathcal{R}_{FVd}$ is the result of adding the power factor constraints 47 and 48 and corresponds to the new IV-ACOPF formulation. This very intuitive ("crust of a pizza slice") shape, in actuality, is a two-dimensional projection of the multi-dimensional feasible region formed by Eqs. 43, 47, and 48. For simplicity of discussion, the remainder of this paper refers to this multi-dimensional region and its two-dimensional projection interchangeably. Note that the lower

bound constraint makes the feasible region $\mathcal{R}_{FVd}$ non-convex. This is because it is possible to choose two points in the feasible region $\mathcal{R}_{FVd}$ and connect them with a line that leaves the feasible region. From these definitions, it follows that the feasible region of the IV-ACOPF formulation R_F prior to any relaxation is $R_F = \bigcap_{d\in\mathcal{D}} R_{FVd}$.

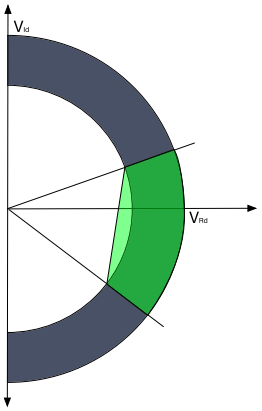

FIGURE 3. Feasible region of the voltage magnitude constraint.

In order to overcome this lack of convexity, this work introduces a high quality relaxation of the feasible region. Graphically, the newly relaxed feasible region $\mathcal{R}_{RF} = \mathcal{R}_F \cup \mathcal{R}_R$ now includes an additional relaxed region $\mathcal{R}_R$ in light green which is formed by the creation of a secant line between the power factor constraints. $\mathcal{R}_R = \bigcap_{d\in\mathcal{D}} \mathcal{R}_{RVd}$.

With respect to the demand bus voltage magnitude lower bounds, they are relaxed to a set of separable secant lines defined by:

$$\left(V_{DR} - \Upsilon_{VDR}\right) = m_{VD} \cdot \left(V_{DI} - \Upsilon_{VDI}\right) \tag{55}$$

where

$$m_{VD} = \frac{\cos(\theta_{VD}^{max}) - \cos(\theta_{VD}^{min})}{\sin(\theta_{VD}^{max}) - \sin(\theta_{VD}^{min})} \tag{56}$$

$$\Upsilon_{VDI} = \underline{|V_D|}\sin(\theta_{VD}^{max}) \tag{57}$$

$$\Upsilon_{VDR} = \underline{|V_D|}\cos(\theta_{VD}^{max}) \tag{58}$$

Note that the secant line is written in the form $V_{DR} = f(V_{DI})$ to avoid the potential for a line with infinite slope.

K. SUMMARY OF IV-ACOPF FORMULATION

The new IV-ACOPF formulation is summarized and recast in the standard form of a convex program.

$$\min \mathcal{J} = \sum_{g\in\mathcal{G}}\left(\alpha_{Zg}(\mathcal{I}_{Rg}^2 + \mathcal{I}_{Ig}^2)^2 + \beta_{Zg}(\mathcal{I}_{Rg}^2 + \mathcal{I}_{Ig}^2) + \gamma_{Rg} + \gamma_{Ig}\right) + \sum_{d\in\mathcal{D}}\left(\bar{\rho}_{Rd}(V_{Rd}I_{Rd} + V_{Id}I_{Id})^2 - \beta_{Rd}(V_{Rd}I_{Rd} + V_{Id}I_{Id}) + \bar{\gamma}_{Rd}\right) + \left(\bar{\rho}_{Id}(-V_{Rd}I_{Id} + V_{Id}I_{Rd})^2 - \beta_{Id}(-V_{Rd}I_{Id} + V_{Id}I_{Rd}) + \bar{\gamma}_{Id}\right) \tag{59}$$

$$s.t. \begin{bmatrix}\mathcal{I}_{GR}\\ -\mathcal{I}_{DR}\end{bmatrix} - \begin{bmatrix}A_G^T\\ A_D^T\end{bmatrix}\mathcal{I}_{LR} = 0 \tag{60}$$

$$\begin{bmatrix}\mathcal{I}_{GI}\\ -\mathcal{I}_{DI}\end{bmatrix} - \begin{bmatrix}A_G^T\\ A_D^T\end{bmatrix}\mathcal{I}_{LI} = 0 \tag{61}$$

$$\begin{bmatrix}A_G^T\\ A_D^T\end{bmatrix}\mathcal{I}_{LR} - G\begin{bmatrix}V_{GR}\\ V_{DR}\end{bmatrix} + B\begin{bmatrix}V_{GI}\\ V_{DI}\end{bmatrix} = 0 \tag{62}$$

$$\begin{bmatrix}A_G^T\\ A_D^T\end{bmatrix}\mathcal{I}_{LI} - B\begin{bmatrix}V_{GR}\\ V_{DR}\end{bmatrix} - G\begin{bmatrix}V_{GI}\\ V_{DI}\end{bmatrix} = 0 \tag{63}$$

$$V_{I_{ref}} = 0 \tag{64}$$

$$\mathcal{I}_{GR} - \mathcal{I}_{GR}^{max} \le 0 \tag{65}$$

$$\mathcal{I}_{GR}^{min} - \mathcal{I}_{GR} \le 0 \tag{66}$$

$$\mathcal{I}_{GI} - \mathcal{I}_{GI}^{max} \le 0 \tag{67}$$

$$\mathcal{I}_{GI}^{min} - \mathcal{I}_{GI} \le 0 \tag{68}$$

$$\mathcal{I}_{LR}^2 + \mathcal{I}_{LI}^2 - |\overline{I_L}|^2 \le 0 \tag{69}$$

$$V_{DR}^2 + V_{DI}^2 - |\overline{V_D}|^2 \le 0 \tag{70}$$

$$V_{DI} - V_{DR}\tan(\theta_{VD}^{max}) \le 0 \tag{71}$$

$$V_{DR}\tan(\theta_{VD}^{min}) - V_{DI} \le 0 \tag{72}$$

$$V_{GR}^2 + V_{GI}^2 - |\overline{V_G}|^2 \le 0 \tag{73}$$

$$\mathcal{I}_{LI} - \mathcal{I}_{LR}\tan(\theta_L^{max}) \le 0 \tag{74}$$

$$\mathcal{I}_{LR}\tan(\theta_L^{min}) - \mathcal{I}_{LI} \le 0 \tag{75}$$

$$\left(V_{DR} - \Upsilon_{VDR}\right) - m_{VD}\left(V_{DI} - \Upsilon_{VDI}\right) \le 0 \tag{76}$$

where the convex constraint in Eq. 76 is the relaxation the non-convex constraint

$$-V_{DR}^2 - V_{DI}^2 + \underline{|V_D|^2} \le 0 \tag{77}$$

It is worth emphasizing that the objective function is separable with respect to each of the generators and demand buses.

$$\mathcal{J} = \sum_{g\in\mathcal{G}} \mathcal{J}_g(\mathcal{I}_{Rg}, \mathcal{I}_{Ig}) + \sum_{d\in\mathcal{D}} \mathcal{J}_d(V_{Rd}, V_{Id}) \tag{78}$$

Meanwhile, with the exception of the network flow constraints in Eq. 60-63, all of the constraints are separable with respect to generators and demand buses as well.

L. CONVEXITY ANALYSIS OF THE FINAL FORMULATION

In order to develop a solution algorithm in the following section, a convexity proof is provided.

Theorem 1: The optimization program described by the objective function 59 and subject to constraints 60-76 is a convex optimization program.

Proof: The objective function as expressed in Eq. 59 is a sum of separable functions of the generator current variables and the demand bus voltage variables. Therefore, the convexity of each of these can be determined independently. The generator cost terms take the form $\sum_g f_g(h_g(\mathcal{I}_{Rg}, \mathcal{I}_{Ig}))$. $h_g()$ is stated in terms of two variables and has a Hessian

whose determinant is equal to 4 and is therefore convex. f_g is stated as a quadratic polynomial of one variable with a leading positive coefficient and therefore is also convex. Because f_g is convex and h_g is convex then the generator cost terms together form a convex function. The demand-bus revenue terms take the form $\sum_d f_d(h_d(V_{Rd}, V_{Id}))$. h_d is an affine map. f_d is a sum of two quadratic polynomials of one variable with a leading positive coefficient and therefore is convex. The composition of a convex function with an affine map is also convex. Eqs. 69-73 are all stated in terms of two (separable) variables and have Hessians whose determinant is equal to 4. The remaining constraints are all linear and create a convex polyhedral feasible region. Therefore, they are convex as well. Because all the constraints are convex and the objective function is convex, the optimization program is also convex. □

IV. NEWTON-RAPHSON (NR) SOLUTION ALGORITHM FOR THE IV-ACOPF FORMULATION

This section presents a Newton-Raphson Solution Algorithm for the *unrelaxed* IV-ACOPF formulation to *global optimality in polynomial time*. First, Theorem 1 provides a solid foundation upon which to solve the *relaxed* IV-ACOPF via Newton-Raphson gradient descent to a candidate solution $y^\dagger$. If $y^\dagger$ is found within the (unrelaxed) feasible $\mathcal{R}_F$, then the algorithm has found a global solution. If $y^\dagger$ is found within the relaxed region $\mathcal{R}_R$, then it must be discarded as infeasible because the $\mathcal{R}_F$ (as we prove below) is infeasible.

To begin, because the *relaxed* IV-ACOPF is a convex optimization program and fulfills Slater's Condition [100], it may be solved straightforwardly by formulating the Lagrangian, deriving the first order optimality (KKT - Karush-Kuhn-Tucker) conditions, and solving using a Newton-Raphson algorithm. The standard form of a convex optimization program is:

$$\text{Minimize} \quad \mathcal{J}(x) \tag{79}$$
$$\text{s.t} \quad h(x) = 0 \tag{80}$$
$$g(x) \leq 0 \tag{81}$$

where $\mathcal{J}(x)$ and $g(x)$ are convex functions and $h(x)$ is an affine function. In this work, $x = [V_{RG}; V_{IG}; I_{RG}; I_{IG}; V_{RD}; V_{ID}]$. Furthermore, h(x) is represented by Equations 60 - 64 and g(x) is represented by Equations 65 - 76. The Lagrangian is:

$$\mathcal{L}(y) = f(x) + \lambda^T h(x) + \mu^T g(x) \tag{82}$$

where $y = [x; \lambda; \mu]$. The first order (KKT) optimality conditions follow straightforwardly from $\nabla\mathcal{L}$.

$$\nabla f(x) + \mu^T \nabla g(x) + \lambda^T \nabla h(x) = 0 \tag{83}$$
$$h(x) = 0 \tag{84}$$
$$g(x) \leq 0 \tag{85}$$
$$\mu \geq 0 \tag{86}$$
$$\mu^T g(x) = 0 \tag{87}$$

where Eq. 83 is the stationarity condition, Eq. 84 and 85 assure primal feasibility, Eq. 86 assures dual feasibility, and Eq. 87 assures complementary slackness. Finally, the Newton-Raphson Algorithm 1 is applied with H_k as the k^{th} iterate of the Hessian of the Lagrangian.

Algorithm 1 Newton-Raphson Minimization Algorithm for Unrelaxed IV-ACOPF Formulation

```
procedure ACOPF(k = 0, y_0, ϵ)
    while ||∇L(y_i)|| < ϵ do
        y_{k+1} ← y_k + H_k^{-1} ∇L(y_k)
        k ← k + 1
    end while
    y† ← y_k
    if y† ∈ R_F then
        y* ← y†
    else
        y* ← ∅
    end if
    return y*
end procedure
```

Theorem 2: Algorithm 1 converges quadratically to a globally optimal solution to the *unrelaxed* IV-ACOPF formulation (defined by Eqs 59-72 and 77) in polynomial-time.

Proof: At a high level, Algorithm 1 is composed of two subsections. In the first, the While Loop implements the well-known Newton-Raphson algorithm to produce the candidate solution $y^\dagger$. The algorithm has a quadratic convergence rate [100] and gives a globally optimal solution to convex optimization problems in polynomial time [110]–[112]. In the second subsection, a test is made on the candidate solution. If $y^\dagger \in \mathcal{R}_F$, then the Newton-Raphson algorithm has found the global optimum. In all other cases, $y^\dagger \in \mathcal{R}_\mathcal{R}$ then by Lemma 1 (below), $\mathcal{R}_F = \emptyset$ and the candidate solution $y^\dagger$ must be discarded and an infeasible solution returned instead. Therefore, Algorithm 1 either finds the globally optimal solution or infeasible solution in polynomial time. □

Lemma 1: If Algorithm 1 returns a candidate solution $y^\dagger \in \mathcal{R}_R$, then $\mathcal{R}_F = \emptyset$.

Proof: A proof by contradiction is is provided. Assume that $\mathcal{R}_F \neq \emptyset$.

1) First recognize that Algorithm 1 *always* returns $|V_G^\dagger| = \overline{|V_G|}$. Because the objective function must minimize generator currents $\mathcal{I}_G$ without consideration for generator terminal voltages, the generator terminal voltages, by Ohm's Law, must rise to their maximal value.
2) In the meantime, an increase of demand-bus voltage magnitudes from $|V_D^\dagger|$ to a hypothetical value $|V_D^\ddagger| = |V_D^\dagger + \Delta V_D|$ where $|\Delta V_D| > 0$ so that $\underline{|V_D|} \leq |V_D^\ddagger| \leq \overline{|V_D|}$, by Lemma 2 (below), *necessitates* an increase in one or more generator voltage magnitudes from $|V_G^\dagger|$ to $|V_G^\ddagger| = |V_G^\dagger + \Delta V_G|$. Because $|V_G^\dagger| = \overline{|V_G|}$, $|V_G^\ddagger| > \overline{|V_G|}$ creates a contradiction where the generator terminal voltage upper bound is violated.

Therefore, by contradiction, if $y^{\dagger} \in \mathcal{R}_R$, then $\mathcal{R}_F = \emptyset$. □

The importance of Lemma 1 to Theorem 2 (as the main result of the paper) cannot be understated. Because this paper uses a steady-state current injection model, it has generator terminal voltages. These generator terminal voltages, in turn, have upper bounds. Any effort to move the demand-bus voltage magnitudes upwards will require the generator terminal voltage magnitudes to move upward as well, and beyond their upper bound values. Therefore, if the demand-bus voltage magnitudes are lower than the lower bounds, then there is no way to increase them without violating the generator terminal voltage upper bounds instead. The reader will recognize that the argument of the Lemma 1 proof presented above is built upon a physical intuition rooted in Ohm's Law: an increase in one of more demand-bus voltage magnitudes necessitates an increase in one or more generator terminal voltage magnitudes. Practicing electrical engineers will recognize this physical intuition as always true by experience. Nevertheless, for a purely mathematical argument, this statement is recast as Lemma 2 below.

Lemma 2: An increase of demand-bus voltage magnitudes from $|V_D^{\dagger}|$ to a hypothetical value $|V_D^{\ddagger}| = |V_D^{\dagger} + \Delta V_D|$ where $|\Delta V_D| > 0$ *necessitates* an increase in one or more generator voltage magnitudes from $|V_G^{\dagger}|$ to $|V_G^{\ddagger}| = |V_G^{\dagger} + \Delta V_G|$.

Proof: A proof by contradiction is provided. First, for simplicity, Equations 10, 11, 18 and 19 are combined into a single linear matrix equality over complex numbers

$$\begin{bmatrix} \mathcal{I}_G^{\dagger} \\ -\mathcal{I}_D \end{bmatrix} = Y \begin{bmatrix} V_G^{\dagger} \\ V_D^{\dagger} \end{bmatrix} = \begin{bmatrix} Y_{GG} & Y_{GD} \\ Y_{DG} & Y_{DD} \end{bmatrix} \begin{bmatrix} V_G^{\dagger} \\ V_D^{\dagger} \end{bmatrix} \tag{88}$$

where the bus admittance matrix $Y = G + jB$ is partitioned into $Y_{GG} = [A_G^T Y_L A_G]$, $Y_{GD} = [A_G^T Y_L A_D]$, $Y_{DG} = [A_D^T Y_L A_G]$, and $Y_{DD} = [A_D^T Y_L A_D]$. Taking the gradient of both sides yields:

$$\begin{bmatrix} \Delta\mathcal{I}_G \\ 0 \end{bmatrix} = \begin{bmatrix} Y_{GG} & Y_{GD} \\ Y_{DG} & Y_{DD} \end{bmatrix} \begin{bmatrix} \Delta V_G \\ \Delta V_D \end{bmatrix} \tag{89}$$

If we assume $\Delta V_G = 0$, then $0 = Y_{DD}\Delta V_D$. Because Y_{DD} is invertible, the only solution to this equation is $\Delta V_D = 0$. $|\Delta V_D| > 0$ is impossible. Therefore, by contradiction, a demand bus voltage increment $|\Delta V_D| > 0$ necessitates a generator terminal voltage increment *magnitude* $|\Delta V_G| > 0$. Finally, a "real-life" electric power system has power lines with positive resistances and reactances. Therefore, $G(i,j) > 0\ \forall i = j$, $G(i,j) \leq 0\ \forall i \neq j$, $B(i,j) < 0\ \forall i = j$, and $B(i,j) \geq 0\ \forall i \neq j$. Therefore, the *direction* of the voltage magnitude increment $|\Delta V_G|$ necessitates an *increase* one or more generator voltage magnitudes from $|V_G^{\dagger}|$ to $|V_G^{\ddagger}| = |V_G^{\dagger} + \Delta V_G|$. □

V. NUMERICAL DEMONSTRATION

To demonstrate the profit-maximizing security-constrained IV-ACOPF, a modified version of the Saadat (1999) transient stability test case [94] is chosen. The associated one-line diagram is shown in Fig. 4. The system consists of three generator buses (in blue) and three generator lead-lines (in red), six demand buses (in green) and seven power lines (in blue). Impedance values have been retained from the original text, and the current withdrawals at the demand buses are shown on the figure. Similarly, the minimum and maximum limits on generator current injections are provided. All bus voltage magnitudes have a lower bound of 0.9 and upper bound of 1.1. The voltage stability constraint limits the angle associated with the current injected to a line between ±20°. A minimum power factor of 0.95 is used to calculate the lower limit on the demand bus voltage phase angle according to Eq. 48. The reference bus is chosen to have the largest voltage phase angle. Therefore, $\theta_{VD}^{max} = 0$. All provided values are given per unit. The chosen marginal cost ($\$/MW$) for each generator and marginal revenue values for each demand-bus are shown in Table 1.

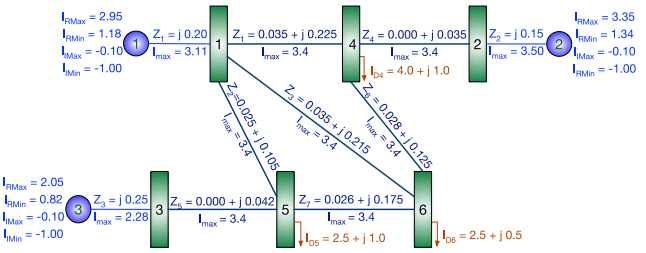

FIGURE 4. Saadat's (1999) Six Demand-Bus, Three Generator Transient Stability Test Case [94]. The topological arrangement and impedance values have been retained. Real and imaginary generator current injection are shown in green.

TABLE 1. Generator & Demand-Bus Revenue Parameters.

Generator	α_{Zg}	β_{Zg}	γ_g			
1	0.2	2	10			
2	0.1125	1.5	10			
3	0.3125	2.5	10			
Demand Bus	$\overline{\rho}_{Rd}$	β_{Rd}	$\overline{\gamma}_{Rd}$	$\overline{\rho}_{Id}$	β_{Id}	$\overline{\gamma}_{Id}$
1	0.25	22	130	0.025	2.2	13
2	0.30	23	130	0.030	2.3	13
3	0.26	25	130	0.026	2.5	13
4	0.28	30	130	0.028	3.0	13
5	0.20	21	130	0.020	2.1	13
6	0.29	19	130	0.029	1.9	13

These input values constitute moderate loading conditions. Here, the IV-ACOPF optimization program reaches a global optimum of $\mathcal{J} = \$763.79$. The associated decision variables are shown in Figure 5. The generators current injections remain well within their real current capacity constraints. That said, Generator 1 has reached its limit with respect to its imaginary current capacity. In the meantime, and as expected, the generator voltage magnitudes are all situated on their respective upper bounds. This is because the IV-ACOPF minimizes the cost of generator current injections but does not depend on generator voltages. Therefore, generator voltages will tend to rise in order to minimize the generator currents. At these moderate loading conditions, all

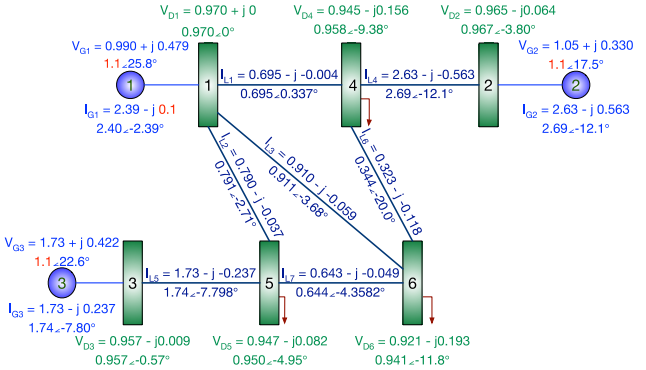

FIGURE 5. Solution of the IV-ACOPF formulation under moderate loading conditions.

of the electric power lines (including generator lead lines) remain unconstrained as well. Finally, all of the demand bus voltages are well within their voltage magnitude constraints. This rather "uneventful" scenario, nevertheless, provides an important result. Under these moderate conditions, the optimum of the relaxed IV-ACOPF is equivalent to the global optima of the unrelaxed problem. Furthermore, because there is a tendency towards higher generator terminal voltages, candidate optimal solutions $y^{\dagger} \in \mathcal{R}_R$ will tend to occur only when necessary, and more specifically under relatively high loading conditions. Reconsider Ohm's Law in Eq. 14. Multiplying on both sides by A_D^T and solving for V_D gives:

$$V_D = -A_1 \mathcal{I}_D - A_2 V_G \tag{90}$$

where

$$A_1 = (A_D^T Y_L A_D)^{-1} \tag{91}$$

$$A_2 = A_1 A_D^T Y_L A_G \tag{92}$$

In short, the network flow constraints can be rearranged so that the demand-bus voltages are written in terms of the demanded currents $\mathcal{I}_D$ and the generator terminal voltages V_G. As $\mathcal{I}_D$ increases, it pulls down demand bus voltages with it.

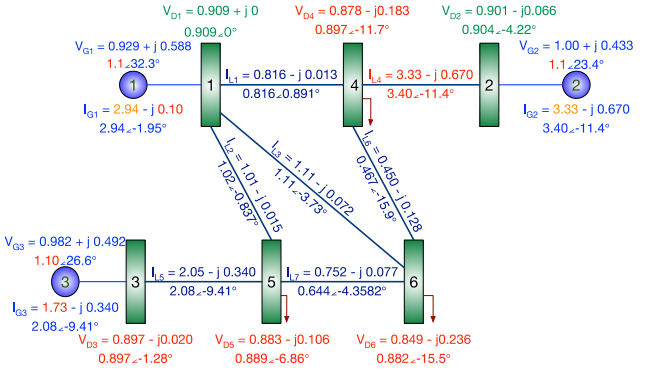

FIGURE 6. The candidate solution $y^{\dagger}$ of the IV-ACOPF formulation under high loading conditions. Because the candidate solution violates the voltage magnitude lower bound constraint, the solution must be discarded and the optimization problem pronounced as infeasible.

A second IV-ACOPF scenario that reflects high loading conditions is now studied. This time, all currents have been increased by 23.3%. Now the IV-ACOPF optimization program reaches an optimum of $\mathcal{J} = \$757.56$. The associated decision variables are shown in Figure 6. In this scenario, Generator 3 has reached its real current capacity limit, while Generators 1 and 2 respectively are less than 1% and 2% away from their real current inject limits. Generator 1 continues to reach its imaginary current capacity limit. Again, as expected, the generator voltage magnitudes are all situated on their respective upper bounds. At these high loading conditions, Power Line 4 has reached its thermal capacity limit. Finally, because of the voltage magnitude relaxation, the voltage magnitudes for demand buses 3, 4, 5 and 6 are now all below the safe value of 0.9p.u by 0.299, 0.307, 1.11, and 1.84% respectively. Therefore, by Lemma 1, this candidate solution must be discarded and the optimization problem pronounced as infeasible. Figure 7 visualizes the candidate solution in a manner similar to that shown in Figure 3.

VI. DISCUSSION: THE IMPORTANCE OF MODELING DECISIONS

This paper has contributed a profit-maximizing security-constrained IV-ACOPF formulation as a convex optimization program which lends itself to a straightforward globally optimal solution via a Newton-Raphson algorithm. In so doing, it has demonstrated several modeling novelties which this section now discusses. The first decision was to switch away from $PQV\theta$ decision variables to IV decision variables. A $PQV\theta$ formulation inevitably introduces non-convex $|V_i||V_j|$ terms ($i \neq j$) in order to calculate the active power P and reactive power Q variables. Similarly, an $IVPQ$ formulation that mixes current, voltage, active power, and reactive power variables must inevitably introduce $S = V \star \mathcal{I}^*$ constraints which are also non-convex. Therefore, a wholehearted flip into IV phasors is required to eliminate these non-convexities. Similarly, the choice of rectangular coordinates for these phasors rather than polar coordinates avoids the introduction of non-convex $\sin(\theta)$ and $\cos(\theta)$ terms. The result is a set of easily managed linear network flow constraints.

This IV-ACOPF also features a steady-state current injection model that includes generator terminals and their associated lead lines. This modeling decision has two primary advantages. First, the power flow analysis assumes complex power injections from generators; that when converted to IV variables imply that the generators are *current sources*. This modeling assumption is physically inconsistent with other electric machine models and power systems engineering models where generators are typically modeled as Thevenin-equivalent *voltage sources* [108], [113], [114]. The choice of voltage sources over current sources corrects the underlying *causality* [115], [116] of the system where the generator's current is *drawn* from the network rather than *imposed* by the generator. Second, the introduction of the generator lead lines in the current injection model means that the

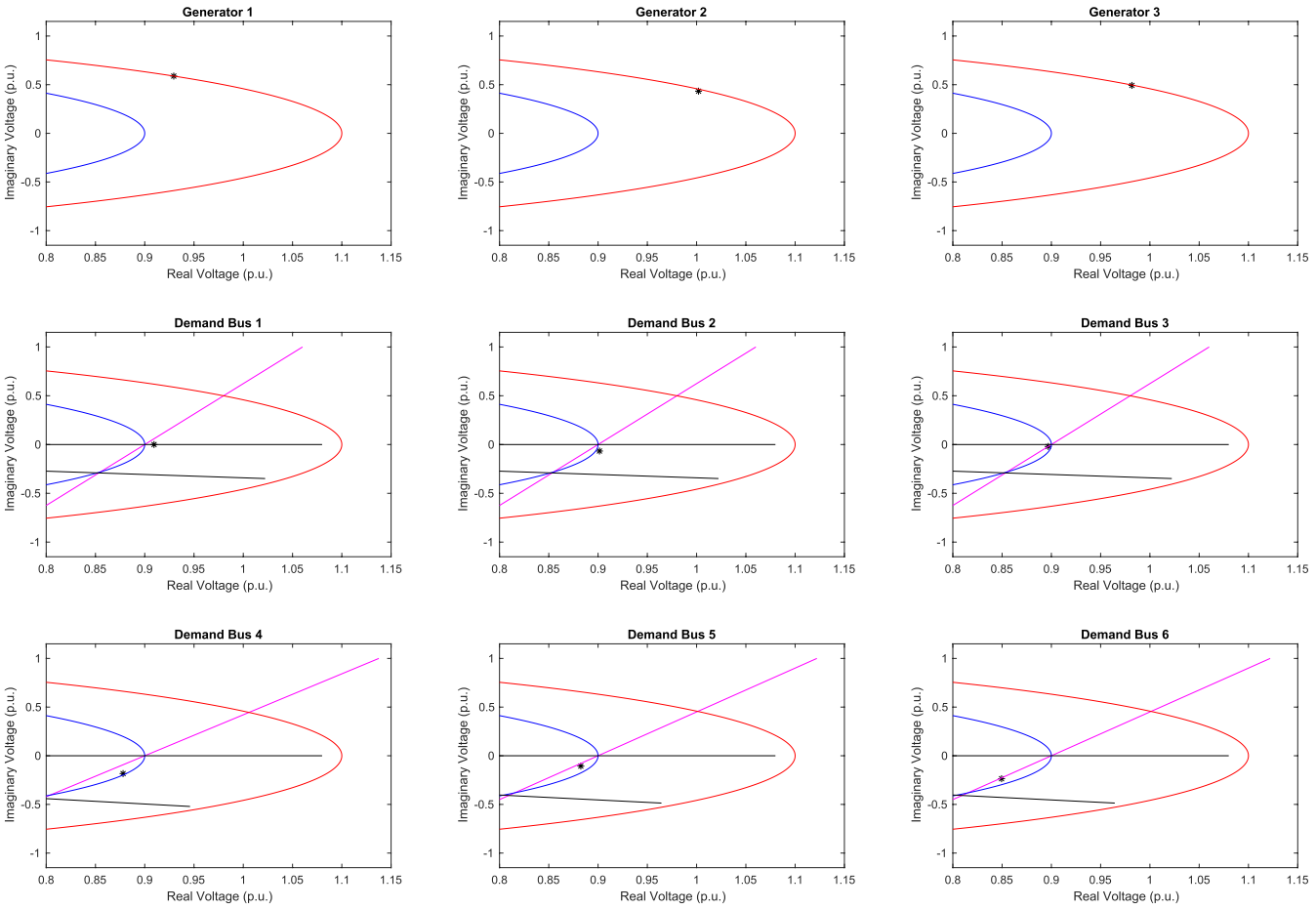

FIGURE 7. The candidate nodal voltage solution $y^{\dagger}$ of the IV-ACOPF formulation under high loading conditions is indicated by *. Voltage upper bounds are shown in red. Voltage lower bounds are shown in blue. Voltage lower bound relaxations are shown in magenta. Power factor upper and lower bounds are shown in black. Each generator and demand bus is shown. Because the candidate solution violates the voltage magnitude lower bound constraint, the solution must be discarded, and the optimization problem pronounced as infeasible.

supply-side of the objective function can now be expressed in terms of generator currents $\mathcal{I}_G$ alone and thus avoid the typical $S = V \star \mathcal{I}^*$ non-convexity when IV formulations must ultimately monetize the purchase and sale of active and reactive power. Said differently, the correction of the physical causality also corrects the mathematical non-convexity.

Along these lines, this IV-ACOPF formulation also takes special care in the design of the objective function. Typical ACOPF formulations that offer a one-sided cost minimization (as in Eq. 9) are just a mathematical short-hand for a two-sided profit maximization with inelastic demand as in Eq. 1. Nevertheless, the distinction in this work is critical because the explicit inclusion of the demand-side revenue terms (even if the demand is inflexible) is instrumental in the derivation of a convex objective function. Although this work continues with the traditional assumption of inelastic demand, this two-sided formulation indicates that one-sided market designs are perhaps outdated and that two-sided markets should become the norm in the context of the 21^{st} century sustainable energy transition. Follow-on works to this paper are likely to investigate elastic demand formulations. The objective function also monetizes both active and reactive power. Because traditional ACOPF formulations have been directed to transmission systems, they have often focused on active power generation and flow and neglected reactive power. In distribution systems, however, the flow of reactive power is often highly constrained. Therefore, this IV-ACOPF formulation provides the monetary incentive to alleviate these reactive power flow constraints. Furthermore, on the demand side, it charges differently for current delivered at one voltage versus another. In conclusion, the objective function gives balanced attention to the supply side, the demand side, active power and reactive power.

This IV-ACOPF formulation also pays special attention to the generator capacity constraints. In that regard, it is clear that the original 1962 paper by Carpentier approximates the capability curve of synchronous generators; which in turn is expressed as a constant voltage multiple of a synchronous generator's phasor diagram. In order to maintain consistency of the modeling, this work simply "undoes"

the multiplication of V_ϕ/X_S but retains the Carpentier's box constraints. This avoids several non-convexities from the synchronous generator's phasor diagram. It also facilitates a market design that is agnostic to device physics and treats all energy resources with the same level playing field; a highly desirable characteristic in the socio-economic design of an equitable electricity market.

The choice of exogeneous data in this IV-ACOPF formulation versus a traditional ACOPF is also of particular importance. The traditional ACOPF provides S_D as exogenous data. When switching to IV variables, this exogeneous data decision reveals two simultaneous dilemmas. First, and mathematically, $S_D = V_D \star \mathcal{I}_D^*$ immediately introduces a constraint of indefinite convexity. Second, and physically, electric power systems are based upon either voltage *or* current *causality*. Introducing exogeneous complex power consumption data S_D is a statement of ambiguous causality of power system physics. When receiving exogeneous data of complex power withdrawals, a power systems engineer should ask whether the underlying physics assumed voltage or current sinks with their associated imposition on causality. In the unlikely event that the load is a voltage sink, then the associated demand-bus voltage decision variable disappears. In contrast, if the load is a current sink (or a given impedance), then the demand-bus voltage remains as a decision variable as provided in this IV-ACOPF formulation. Although, existing ACOPF implementations have amassed considerable quantities of complex power demand data, the original source of this data normally collects the associated current phasor data as well; either from SCADA (Supervisory Control and Data Acquisition) systems or smart meters. Therefore, the benefits of changing exogeneous data from S_D to $\mathcal{I}_D$ greatly outweigh the relatively modest implementation effort. Similarly, existing forecasting software which normally predict S_D can be retooled with historical voltage phasor data V_D to produce $\mathcal{I}_D$. Alternatively, new forecasting software can predict $\mathcal{I}_D$ directly from historical current phasor data. The implementation steps avoid the use complex power data with indefinite convexity *and* ambiguous physical causality.

Finally, it is important to comment on the equivalence of this IV-ACOPF to the original ACOPF problem described in Sec. II.

Theorem 3: Given the optimal vector of demand-bus voltage phasors $V_D^\dagger$, the IV-ACOPF formulation defined by Equation 59-72 and 77 is a *generalization* of the ACOPF formulation defined by Equations 1-8 when P_D and $\mathcal{I}_D^*$ are chosen such that $S_D = V_D^\dagger \mathcal{I}_D^*$.

Proof: The equations of the IV-ACOPF are addressed in turn.

- By the discussion in Section III-C, the objective function in Eq. 59 is equivalent to Eq. 1 when $\alpha_{Ig} = \alpha_{Id} = \beta_{Ig} = \beta_{Id} = 0 \quad \forall g \in \mathcal{G}, d \in \mathcal{D}$.
- From the proof of Lemma 2, the network flow equations 60-63 are combined to yield Equation 88. Applying the definitions of Y_L, A_G and A_D to the bottom block-row of equations gives:

$$-\mathcal{I}_D = A_{DG}^T Y_{LG} A_{GG} V_G + A_{DG}^T Y_{LG} A_{DG} V_D + A_{DD}^T Y_{LD} A_{DD} V_D \quad (93)$$

Substituting in Ohm's Law on the lead lines from Eq. 15 and the definition of a bus admittance matrix $Y_D = Y_{LD}^T A_{DD} V_D$ gives:

$$-\mathcal{I}_D = A_{DG}^T I_{LG} + Y_{DD} V_D \quad (94)$$

This same result can be confirmed from the power analysis model by rewriting Equations 2 and 3 in complex matrix form:

$$A_{GD} S_G - S_D = diag(V_D) Y_D^* V_D^* \quad (95)$$

and then dividing all terms by $diag(V_D)$. Because S_D and $\mathcal{I}_D$ are exogeneous constants they must be related by the optimal vector of demand-bus voltage phasors $V_D^\dagger$. $S_D = V_D^\dagger \mathcal{I}_D^*$.

- By the discussion in Section III-D, the reference angle constraint in Eq. 64 is equivalent to Eq. 4.
- By the discussion in Section III-E, the generator capacity constraints in Equations 65 - 68 are equivalent to Equations 5 and 6.
- By the discussion in Section III-F, the thermal line flow constraint in Eq. 69 is equivalent to Eq. 7.
- By the discussion in Section III-G, the voltage magnitude constraints in Equations 73 and 77 are equivalent to Eq. 8.
- By the discussion in Section III-H, the exogeneous constant $S_D = P_D + jQ_D$ in the ACOPF is a specific condition of the power factor upper and lower bounds in Equations 71 and 72 where $\theta_{VD}^{max} = \theta_{VD}^{min}$ and $\theta_{VD} - \theta_{ID} = \tan^{-1}(Q_D/P_D)$. □

Note that Theorem 3 omits the generator terminal voltage upper bound because the generator terminals do not appear in the power flow analysis model of the ACOPF. Their re-inclusion serves to protect generators from over-voltages. Similarly, the theorem omits the voltage stability constraints in Equations 74 and 75 because they do not appear in the original ACOPF either. Their re-inclusion would protect the grid from voltage instabilities. Lastly, the voltage magnitude lower bound relaxation in Eq. 76 is superfluous in the presence of the more binding voltage magnitude lower bound in Eq. 77. In other words, and as a significant conclusion of this paper, when P_D and $\mathcal{I}_D^*$ are chosen such that $P_D = V_D^\dagger \mathcal{I}_D^*$ and $\alpha_{Ig} = \alpha_{Id} = \beta_{Ig} = \beta_{Id} = 0 \quad \forall g \in \mathcal{G}, d \in \mathcal{D}$, then the optimal point $x^* = [V_{RG}; V_{IG}; I_{RG}; I_{IG}; V_{RD}; V_{ID}]$ of the IV-ACOPF formulation defined by Equation 59-72 and 77 is equivalent to optimum point $\chi = [P_G; Q_G; |V_D|; \theta_D]$ from the ACOPF formulation defined by Equations 1-8.

Beyond these equivalence conditions, it is important to recognize that the more general conditions of the IV-ACOPF offer notable improvements. More specifically, relaxing the condition $P_D = V_D^\dagger \mathcal{I}_D^*$ means that the demand side is no longer a constant but rather a *function* of demand-bus

voltages. The original ACOPF 1.) ignores the demand side entirely and 2.) does not differentiate between the sale of electric power at one voltage versus another (assuming, perhaps incorrectly, that a customer is indifferent to voltage magnitude). Instead, the inclusion of these demand side terms as functions in the IV-ACOPF explicitly differentiates the sale of electric power at one voltage versus another. In a 21^{st} century sustainable energy transition characterized by the energy Internet of Things [36] and other demand side resources [117], it is likely that treating the sale of only active power integrated over time on a purely kWh basis irrespective of voltage level is no longer viable in the long-term. Furthermore, the use of exogeneous power demand data S_D was an immediate source of indefinite convexity *and* was an immediate source of ambiguous physical causality. The switch to exogeneous current demand $\mathcal{I}_D$ data alleviates both of these problems and a practical power systems engineer may ask why the (original) ACOPF should continue to be solved in light of these problems with S_D as the choice of exogeneous data. Setting aside these computational and practical benefits, in the end, the IV-ACOPF and ACOPF models both effectively secure the grid. While the IV-ACOPF formulation can be solved to global optimality in polynomial time, the original ACOPF, at present, can not.

VII. CONCLUSION

In conclusion, this paper has contributed a profit maximizing security-constrained current-voltage AC optimal power flow (IV-ACOPF) model and globally optimal algorithm. The main novelty of the work is its exclusive use of current and voltage phasors in rectangular coordinates to maintain the convexity of the optimization problem. The formulation also explicitly includes both the supply and demand sides to provide a profit maximizing rather than cost minimizing functionality. The now linear network flow constraints also facilitate the inclusion of power factor constraints (Eq. 47 and 48) and voltage stability constraints (Eq. 53 and 54) that are often neglected in typical optimal power flow formulations. This IV-ACOPF does feature a high quality ''secant-line'' relaxation on the otherwise non-convex voltage magnitude lower bound. This new IV-ACOPF reformulation facilitates a straightforward polynomial-time globally optimal solution via a Newton-Raphson algorithm. The numerical results confirm the globally optimal solution and return infeasible solutions when the loading conditions are excessively high. As elaborated in the discussion section, this paper opens the door to significant future work that enables the sustainable energy transition; including application to the operation of distribution systems and microgrids, two-sided markets with elastic demand, and coupling to other infrastructure sectors. It also is likely to have direct application to generation and transmission planning methods.

ACKNOWLEDGMENT

The authors would like to thank Prof. Kamal Youcef-Toumi, Prof. Massoud Amin, and Prof. Scott Moura for graciously reading and commenting on the work prior to its publication in IEEE Access., and their would also like to thank the anonymous IEEE Access reviewers for their suggestions on the clarity of the work.

NOMENCLATURE

DECISION VARIABLES

$\mid V_D \mid$	Magnitudes of Voltage Phasors for Demand Buses.
θ_{ID}	Phase Angle of Current Phasor for Demand Buses.
θ_{VD}	Phase Angle of Voltage Phasor for Demand Buses.
θ_{VD}^{max}	Upper Bound on Phase Angle of Voltage Phasor for Demand Buses.
θ_{VD}^{min}	Lower Bound on Phase Angle of Voltage Phasor for Demand Buses.
J	Profit Objective Functin.
MC_G	Marginal Revenue.
MR_D	Marginal Cost.
P_G	Active Power from Generators.
P_L	Active Power through Power Lines.
Q_G	Reactive Power from Generators.
Q_L	Reactive Power through Power Lines.
S_G	Complex Power from Generators.
S_L	Complex Power through Power Lines.
V_{DI}	Imaginary Part of Voltage Phasors for Demand Buses.
V_{DR}	Real Part of Voltage Phasors for Demand Buses.
V_D	Voltage Phasors for Demand Buses.
V_{GI}	Imaginary Part of Voltage Phasors for Generators.
V_{GR}	Real Part of Voltage Phasors for Generators.
V_G	Voltage Phasors for Generators.
$\mathcal{I}_{\mathcal{LDI}}$	Imaginary Part of Current Phasors for Demand Bus to Demand Bus Power Lines.
$\mathcal{I}_{\mathcal{LDR}}$	Real Part of Current Phasors for Demand Bus to Demand Bus Power Lines.
$\mathcal{I}_{\mathcal{LD}}$	Current Phasors for Demand Bus to Demand Bus Power Lines.
$\mathcal{I}_{\mathcal{LGI}}$	Imaginary Part of Current Phasors for Generator Lead Lines.
$\mathcal{I}_{\mathcal{LGR}}$	Real Part of Current Phasors for Generator Lead Lines.
$\mathcal{I}_{\mathcal{LG}}$	Current Phasors for Generator Lead Lines.
$\mathcal{I}_{\mathcal{LI}}$	Imaginary Part of Current Phasors for Power Lines.
$\mathcal{I}_{\mathcal{LR}}$	Real Part of Current Phasors for Power Lines.
$\mathcal{I}_{\mathcal{L}}$	Current Phasors for Power Lines.
$\mathcal{I}_{GI}$	Imaginary Part of Current Phasors for Generators.
$\mathcal{I}_{GR}$	Real Part of Current Phasors for Generators.
$\mathcal{I}_G$	Current Phasors for Generators.

OTHER SYMBOLS

$f()$	A Generic Function.
$g()$	A Generic Function.
$h()$	A Generic Function.
k	Iteration Counter.
$y^{\dagger}$	A Candidate Solution.

$y^{\dagger}$	An Optimal Solution.
$\mathcal{L}()$	A Lagrangian Function.
λ	Lagrange Multiplies.
λ_e	Eigenvalues.

PARAMETERS

α_{R_D}	Quadratic Cost Coefficient for Active Power from Demand Buses.
α_{R_G}	Quadratic Cost Coefficient for Active Power from Generators.
β_{R_D}	Linear Cost Coefficient for Active Power from Demand Buses.
β_{R_G}	Linear Cost Coefficient for Active Power from Generators.
γ_{R_D}	Fixed Cost Coefficient for Active Power from Demand Buses.
γ_{R_G}	Fixed Cost Coefficient for Active Power from Generators.
$\mid V_D \mid^{max}$	Upper Bound on Voltage Magnitude of Demand Buses.
$\mid V_D \mid^{min}$	Lower Bound on Voltage Magnitude of Demand Buses.
A_D	Line-to-Bus Incidence Matrix.
A_{GD}	Generator-to-Demand Bus Incidence Matrix.
A_G	Line-to-Generator Incidence Matrix.
B	Bus Susceptance Matrix.
B_L	Generator & Bus Susceptance Matrix.
G	Bus Conductance Matrix.
G_L	Generator & Bus Conductance Matrix.
$N_{\mathcal{D}}$	Number of Demand Buses.
$N_{\mathcal{D}}$	Number of Power Lines.
$N_{\mathcal{G}}$	Number of Generators.
P_D	Active Power from Demand Buses.
P_G^{max}	Upper Bound on Active Power from Generators.
P_G^{min}	Lower Bound on Active Power from Generators.
P_L^{max}	Upper Bound on Active Power through Power Lines.
Q_D	Reactive Power from Demand Buses.
Q_G^{max}	Upper Bound on Reactive Power from Generators.
Q_G^{min}	Lower Bound on Reactive Power from Generators.
S_D	Complex Power from Demand Buses.
Y	Bus Admittance Matrix.
Y_L	Generator & Bus Admittance Matrix.
$\mathcal{I}_{DI}$	Imaginary Part of Current Phasors for Demand Buses.
$\mathcal{I}_{DR}$	Real Part of Current Phasors for Demand Buses.
$\mathcal{I}_D$	Current Phasors for Demand Buses.
$\mathcal{Y}_L$	Lead Line and Power Line Admittances.

SETS

$d \in \mathcal{D}$	Demand Buses.
$g \in \mathcal{G}$	Generators.
$l \in \mathcal{L}$	Power Lines.
$l \in \mathcal{L}_D$	Demand Bus to Demand Bus Power Lines.
$l \in \mathcal{L}_G$	Generator Lead Lines.
$\mathcal{R}_F$	Feasible Region.
$\mathcal{R}_{RF}$	Relaxed Feasible Region.
$\mathcal{R}_R$	Relaxed Region.

REFERENCES

[1] J. Carpentier, "Contribution to the economic dispatch problem," *Bull. Soc. Franc. Electr.*, vol. 3, no. 8, pp. 431–447, 1962.

[2] S. Frank and S. Rebennack, "A primer on optimal power flow: Theory, formulation, and practical examples," Colorado School of Mines, Golden, CO, USA, Tech. Rep. 2012-14, Oct. 2012, pp. 1–42.

[3] M. Cain, R. O'neill, and A. Castillo, "History of optimal power flow and formulations," Federal Energy Regulatory Commission, Washington, DC, USA, Tech. Rep. 1, 2012, pp. 1–36.

[4] A. Muzhikyan, S. O. Muhanji, G. D. Moynihan, D. J. Thompson, Z. M. Berzolla, and A. M. Farid, "The 2017 ISO new England system operational analysis and renewable energy integration study (SOARES)," *Energy Rep.*, vol. 5, pp. 747–792, Nov. 2019, doi: 10.1016/j.egyr.2019.06.005.

[5] *PJM Manual 11: Energy and Ancillary Services Market Operations*, PJM, Norristown, PA, USA, Oct. 2012.

[6] A. Garcia, L. Mili, and J. Momoh, "Modeling electricity markets: A brief introduction," in *Economic Market Design and Planning for Electric Power Systems*. Hoboken, NJ, USA: Wiley, 2009, pp. 21–44, doi: 10.1002/9780470529164.ch2.

[7] J. J. Shaw, "A direct method for security-constrained unit commitment," *IEEE Trans. Power Syst.*, vol. 10, no. 3, pp. 1329–1342, Aug. 1995.

[8] J. Wang, M. Shahidehpour, and Z. Li, "Security-constrained unit commitment with volatile wind power generation," *IEEE Trans. Power Syst.*, vol. 23, no. 3, pp. 1319–1327, Aug. 2008.

[9] J. D. Guy, "Security constrained unit commitment," *IEEE Trans. Power App. Syst.*, vol. PAS-90, no. 3, pp. 1385–1390, 1971.

[10] M. Vahedipour-Dahraei, H. R. Najafi, A. Anvari-Moghaddam, and J. M. Guerrero, "Security-constrained unit commitment in AC microgrids considering stochastic price-based demand response and renewable generation," *Int. Trans. Electr. Energy Syst.*, vol. 28, no. 9, p. e2596, Sep. 2018.

[11] S. L. Gbadamosi and N. I. Nwulu, "A comparative analysis of generation and transmission expansion planning models for power loss minimization," *Sustain. Energy, Grids Netw.*, vol. 26, Jun. 2021, Art. no. 100456.

[12] N. E. Koltsaklis and A. S. Dagoumas, "State-of-the-art generation expansion planning: A review," *Appl. Energy*, vol. 230, pp. 563–589, Nov. 2018.

[13] C. Li, A. J. Conejo, P. Liu, B. P. Omell, J. D. Siirola, and I. E. Grossmann, "Mixed-integer linear programming models and algorithms for generation and transmission expansion planning of power systems," *Eur. J. Oper. Res.*, vol. 297, no. 3, pp. 1071–1082, Mar. 2022.

[14] M. Moradi-Sepahvand and T. Amraee, "Integrated expansion planning of electric energy generation, transmission, and storage for handling high shares of wind and solar power generation," *Appl. Energy*, vol. 298, Sep. 2021, Art. no. 117137.

[15] D. K. Molzahn, C. Josz, I. A. Hiskens, and P. Panciatici, "A laplacian-based approach for finding near globally optimal solutions to OPF problems," *IEEE Trans. Power Syst.*, vol. 32, no. 1, pp. 305–315, Jan. 2017.

[16] P. P. C. Z. Silano Chen and P. A., "Optimal allocation of wind turbines in active distribution networks by using multi-period optimal power flow and genetic algorithms," in *Proc. Modeling Control Sustain. Power Syst.*, 2012, pp. 1–20.

[17] A. G. Bakirtzis, P. N. Biskas, C. E. Zoumas, and V. Petridis, "Optimal power flow by enhanced genetic algorithm," *IEEE Trans. Power Syst.*, vol. 17, no. 2, pp. 229–236, May 2002.

[18] S. R. Paranjothi and K. Anburaja, "Optimal power flow using refined genetic algorithm," *Electr. Power Compon. Syst.*, vol. 30, no. 10, pp. 1055–1063, Oct. 2002.

[19] M. S. Osman, M. A. Abo-Sinna, and A. A. Mousa, "A solution to the optimal power flow using genetic algorithm," *Appl. Math. Comput.*, vol. 155, no. 2, pp. 391–405, Aug. 2004.

[20] D. Devaraj and B. Yegnanarayana, "Genetic-algorithm-based optimal power flow for security enhancement," *IEE Proc.-Gener., Transmiss. Distrib.*, vol. 152, no. 6, pp. 899–905, Nov. 2005.

[21] U. Leeton, D. Uthitsunthorn, U. Kwannetr, N. Sinsuphun, and T. Kulworawanichpong, "Power loss minimization using optimal power flow based on particle swarm optimization," in *Proc. Int. Conf. onElectr. Eng./Electron. Comput. Telecommun. Inf. Technol. (ECTI-CON)*, 2010, pp. 440–444.

[22] E. Sortomme and M. A. El-Sharkawi, "Optimal power flow for a system of microgrids with controllable loads and battery storage," in *Proc. IEEE/PES Power Syst. Conf. Expo.*, Mar. 2009, pp. 1–5.

[23] M. A. Abido, "Optimal power flow using particle swarm optimization," *Int. J. Elect. Power Energy Syst.*, vol. 24, no. 7, pp. 563–571, 2002.
[24] S. He, J. Y. Wen, E. Prempain, Q. H. Wu, J. Fitch, and S. Mann, "An improved particle swarm optimization for optimal power flow," in *Proc. Int. Conf. Power Syst. Technol. PowerConf.*, 2013, pp. 1–40.
[25] J. Hazra and A. K. Sinha, "A multi-objective optimal power flow using particle swarm optimization," *Eur. Trans. Electr. Power*, vol. 21, no. 1, pp. 1028–1045, Jan. 2011.
[26] C.-R. Wang, H.-J. Yuan, Z.-Q. Huang, J.-W. Zhang, and C.-J. Sun, "A modified particle swarm optimization algorithm and its application in optimal power flow problem," in *Proc. Int. Conf. Mach. Learn. Cybern.*, vol. 5, Aug. 2005, pp. 2885–2889.
[27] R.-H. Liang, S.-R. Tsai, Y.-T. Chen, and W.-T. Tseng, "Optimal power flow by a fuzzy based hybrid particle swarm optimization approach," *Electr. Power Syst. Res.*, vol. 81, no. 7, pp. 1466–1474, 2011.
[28] C. A. Roa-Sepulveda and B. J. Pavez-Lazo, "A solution to the optimal power flow using simulated annealing," *Int. J. Electr. Power Energy Syst.*, vol. 25, no. 1, pp. 47–57, 2003.
[29] T. Sousa, J. Soares, Z. Vale, H. Morais, and P. Faria, "Simulated annealing metaheuristic to solve the optimal power flow," in *Proc. IEEE Power Energy Soc. Gen. meeting*, Apr. 2011, pp. 1–8.
[30] T. Niknam, M. R. Narimani, and M. Jabbari, "Dynamic optimal power flow using hybrid particle swarm optimization and simulated annealing," *Int. Trans. Electr. Energy Syst.*, vol. 23, no. 7, pp. 975–1001, Oct. 2013.
[31] V. J. Gutierrez-Martinez, C. A. Canizares, C. R. Fuerte-Esquivel, A. Pizano-Martinez, and X. Gu, "Neural-network security-boundary constrained optimal power flow," *IEEE Trans. Power Syst.*, vol. 26, no. 1, pp. 63–72, Feb. 2011.
[32] P. Siano, C. Cecati, H. Yu, and J. Kolbusz, "Real time operation of smart grids via FCN networks and optimal power flow," *IEEE Trans. Ind. Informat.*, vol. 8, no. 4, pp. 944–952, Nov. 2012.
[33] X. Pan, T. Zhao, and M. Chen, "DeepOPF: Deep neural network for DC optimal power flow," in *Proc. IEEE Int. Conf. Commun., Control, Comput. Technol. Smart Grids*, Oct. 2019, pp. 1–6.
[34] X. Pan, M. Chen, T. Zhao, and S. H. Low, "DeepOPF: A feasibility-optimized deep neural network approach for AC optimal power flow problems," 2020, *arXiv:2007.01002*.
[35] S. Frank, I. Steponavice, and S. Rebennack, "Optimal power flow: A bibliographic survey II," *Energy Syst.*, vol. 3, no. 3, pp. 259–289, Sep. 2012.
[36] S. O. Muhanji, A. E. Flint, and A. M. Farid, *EIoT: The Development Energy Internet Things Energy Infrastructure*. Berlin, Germany: Springer, 2019, doi: 10.1007/978-3-030-10427-6.
[37] C. Cecati, C. Citro, A. Piccolo, and P. Siano, "Smart grid operation with distributed generation and demand side management," in *Modeling and Control of Sustainable Power Systems*. Berlin, Germany: Springer, 2012, pp. 27–81.
[38] L. Wang, *Modeling and Control of Sustainable Power Systems,Wang and Lingfeng*, L. Wang, Ed. Berlin, Germany: Springer, 2012.
[39] G. Ferruzzi, G. Graditi, F. Rossi, and A. Russo, "Optimal operation of a residential microgrid: The role of demand side management," *Intell. Ind. Syst.*, vol. 1, no. 1, pp. 61–82, Jun. 2015.
[40] D. Gayme and U. Topcu, "Optimal power flow with large-scale storage integration," *IEEE Trans. Power Syst.*, vol. 28, no. 2, pp. 709–717, May 2013.
[41] F. A. Rahimi and A. Ipakchi, "Transactive energy techniques: Closing the gap between wholesale and retail markets," *Electr. J.*, vol. 25, no. 8, pp. 29–35, 2012.
[42] *Pacific Northwest Gridwise Testbed Demonstration Projects: Part 2. Grid-Friendly Appliances Project*, Pacific Northwest Nat. Lab., Richland, WA, USA, 2007.
[43] *Pacific Northwest Gridwise Testbed Demonstration Projects Part 1. Olympic Peninsula Project*, Pacific Northwest Nat. Lab., Richland, WA, USA, 2007.
[44] D. Hammerstrom, R. Ambrosio, J. Brous, T. Carlon, D. Ghassin, J. DeSteese, R. Guttromson, G. Horst, O. Järregren, and R. Kajfasz, "Pacific northwest gridwise TM testbed demonstration projects, volume I: The Olympic peninsula project," Pacific Northwest Nat. Lab., Richland, WA, USA, Tech. Rep. PNNL-17167, 2007.
[45] S. E. Widergren, K. Subbarao, J. C. Fuller, D. P. Chassin, A. Somani, M. C. Marinovici, and J. L. Hammerstrom, "AEP Ohio gridSMART demonstration project real-time pricing demonstration analysis," Pacific Northwest Nat. Lab., Richland, WA, USA, Tech. Rep. 45, 2014.
[46] W.-C. Lin and H. E. Garcia, "Inclusion of game-theoretic formulations for resilient condition assessment monitoring," in *Proc. 6th Int. Symp. Resilient Control Syst. (ISRCS)*, Aug. 2013, pp. 96–103, doi: 10.1109/ISRCS.2013.6623758.
[47] V. Hosseinnezhad, M. Rafiee, M. Ahmadian, and P. Siano, "Optimal day-ahead operational planning of microgrids," *Energy Convers. Manage.*, vol. 126, pp. 142–157, Oct. 2016. [Online]. Available: http://www.sciencedirect.com/science/article/pii/S0196890416306549
[48] E. Dall'Anese, H. Zhu, and G. B. Giannakis, "Distributed optimal power flow for smart microgrids," *IEEE Trans. Smart Grid*, vol. 4, no. 3, pp. 1464–1475, Sep. 2013.
[49] Y. Levron, J. M. Guerrero, and Y. Beck, "Optimal power flow in microgrids with energy storage," *IEEE Trans. Power Syst.*, vol. 28, no. 3, pp. 3226–3234, Aug. 2013.
[50] H. Gao, J. Liu, L. Wang, and Z. Wei, "Decentralized energy management for networked microgrids in future distribution systems," *IEEE Trans. Power Syst.*, vol. 33, no. 4, pp. 3599–3610, Jul. 2018.
[51] *Investor-Owned Utilities Served 72% of U.S. Electricity Customers in 2017*, U.S. Energy Inf. Admin., Washington, DC, USA, Aug. 2019. [Online]. Available: https://www.eia.gov/todayinenergy/detail.php?id=40913
[52] D. Molzahn, F. Dörfler, and H. Sandberg, "A survey of distributed optimization and control algorithms for electric power systems," *IEEE Trans. Smart Grid*, vol. 8, no. 6, pp. 2941–2962, Nov. 2017.
[53] S. O. Muhanji, A. Muzhikyan, and A. M. Farid, "Distributed control for distributed energy resources: Long-term challenges and lessons learned," *IEEE Access*, vol. 6, pp. 32737–32753, 2018, doi: 10.1109/ACCESS.2018.2843720.
[54] S. O. Muhanji, A. Muzhikyan, and A. M. Farid, "Long-term challenges for future electricity markets with distributed energy resources," in *Smart Grid Control: An Overview Res. Opportunities*, J. Stoustrup, A. M. Annaswamy, A. Chakrabortty, and Z. Qu, Eds. Berlin, Germany: Springer, 2017, pp. 59–81, doi: 10.1007/978-3-319-98310-3.
[55] A. Santhosh, A. M. Farid, and K. Youcef-Toumi, "Real-time economic dispatch for the supply side of the energy-water nexus," *Appl. Energy*, vol. 122, pp. 42–52, Jun. 2014, doi: 10.1016/j.apenergy.2014.01.062.
[56] A. Santhosh, A. M. Farid, and K. Youcef-Toumi, "The impact of storage facility capacity and ramping capabilities on the supply side of the energy-water nexus," *Energy*, vol. 66, no. 1, pp. 1–10, 2014, doi: 10.1016/j.energy.2014.01.031.
[57] W. N. Lubega and A. M. Farid, "Quantitative engineering systems modeling and analysis of the energy–water nexus," *Appl. Energy*, vol. 135, pp. 142–157, Dec. 2014, doi: 10.1016/j.apenergy.2014.07.101.
[58] W. Hickman, A. Muzhikyan, and A. M. Farid, "The synergistic role of renewable energy integration into the unit commitment of the energy water nexus," *Renew. Energy*, vol. 108, pp. 220–229, Aug. 2017, doi: 10.1016/j.renene.2017.02.063.
[59] A. M. Farid, "A hybrid dynamic system model for multi-modal transportation electrification," *IEEE Trans. Control Syst. Technol.*, vol. 25, no. 3, pp. 940–951, May 2016, doi: 10.1109/TCST.2016.2579602.
[60] W. C. Schoonenberg and A. M. Farid, "A dynamic model for the energy management of microgrid-enabled production systems," *J. Cleaner Prod.*, vol. 1, no. 1, pp. 1–10, 2017, doi: 10.1016/j.jclepro.2017.06.119.
[61] M. Cvetkovic and A. Annaswamy, "Coupled ISO-NE real-time energy and regulation markets for reliability with natural gas," in *Proc. IEEE Power Energy Soc. Gen. Meeting*, Jul. 2015, pp. 1–5.
[62] C. M. Correa-Posada and P. Sanchez-Martin, "Security-constrained optimal power and natural-gas flow," *IEEE Trans. Power Syst.*, vol. 29, no. 4, pp. 1780–1787, Jul. 2014.
[63] C. Liu, M. Shahidehpour, Y. Fu, and Z. Li, "Security-constrained unit commitment with natural gas transmission constraints," *IEEE Trans. Power Syst.*, vol. 24, no. 3, pp. 1523–1536, Aug. 2009.
[64] T. Li, M. Eremia, and M. Shahidehpour, "Interdependency of natural gas network and power system security," *IEEE Trans. Power Syst.*, vol. 23, no. 4, pp. 1817–1824, Nov. 2008.
[65] E. M. Wanjiru, S. M. Sichilalu, and X. Xia, "Model predictive control of heat pump water heater-instantaneous shower powered with integrated renewable-grid energy systems," *Appl. Energy*, vol. 204, pp. 1333–1346, Oct. 2017.
[66] P. Mancarella, "MES (multi-energy systems): An overview of concepts and evaluation models," *Energy*, vol. 65, pp. 1–17, Feb. 2014.
[67] Z. Li, W. Wu, M. Shahidehpour, J. Wang, and B. Zhang, "Combined heat and power dispatch considering pipeline energy storage of district heating network," *IEEE Trans. Sustain. Energy*, vol. 7, no. 1, pp. 12–22, Jan. 2016.
[68] H. Lund, S. Werner, R. Wiltshire, S. Svendsen, J. E. Thorsen, F. Hvelplund, and B. V. Mathiesen, "4th generation district heating (4GDH): Integrating smart thermal grids into future sustainable energy systems," *Energy*, vol. 68, pp. 1–11, Apr. 2014.

[69] *Nerc White Paper on Ferc Nopr [Docket rm16-1-000] Proposal to Revise Standard Generator Interconnection Agreements*, NERC, Atlanta, GA, USA, 2016.
[70] A. Ellis, R. Nelson, and E. Von Engeln, "Review of existing reactive power requirements for variable generation," in *Proc. IEEE Power Energy Soc. Gen. Meeting*, Apr. 2012, pp. 1–7.
[71] M. Huneault and F. D. Galiana, "A survey of the optimal power flow literature," *IEEE Trans. Power Syst.*, vol. 6, no. 2, pp. 762–770, May 1991.
[72] J. A. Momoh, M. E. El-Hawary, and R. Adapa, "A review of selected optimal power flow literature to 1993. II. Newton, linear programming and interior point methods," *IEEE Trans. Power Syst.*, vol. 14, no. 1, pp. 96–104, Feb. 1999.
[73] J. A. Momoh, R. Adapa, and M. E. El-Hawary, "A review of selected optimal power flow literature to 1993. Iw. Nonlinear and quadratic programming approaches," *IEEE Trans. Power Syst.*, vol. 14, no. 1, pp. 96–104, Feb. 1999.
[74] S. Frank, I. Steponavice, and S. Rebennack, "Optimal power flow: A bibliographic survey I," *Energy Syst.*, vol. 3, no. 3, pp. 221–258, Sep. 2012.
[75] R. P. O'Neill, A. Castillo, and M. B. Cain, "The IV formulation and linear approximations of the AC optimal power flow problem," Federal Energy Regulatory Commission, Washington, DC, USA, Tech. Rep., Dec. 2012.
[76] A. Castillo and R. P. O'Neill, "Survey of approaches to solving the ACOPF," Federal Energy Regulatory Commission, Washington, DC, USA, Tech. Rep., Mar. 2013.
[77] K. Pandya and S. Joshi, "A survey of optimal power flow methods," *J. Theor. Appl. Inf. Technol.*, vol. 4, pp. 450–458, Jan. 2008.
[78] E. Mohagheghi, M. Alramlawi, A. Gabash, and P. Li, "A survey of real-time optimal power flow," *Energies*, vol. 11, no. 11, p. 3142, 2018.
[79] D. Molzahn and I. Hiskens, *A Survey of Relaxations and Approximations of the Power Flow Equations*. Now, 2019, doi: 10.1561/3100000012.
[80] P. Schavemaker and L. Van der Sluis, *Electrical Power System Essentials*. Chichester, U.K.: Wiley, 2008. [Online]. Available: http://www.loc.gov/catdir/enhancements/fy0810/2008007359-d.html
[81] K. Dvijotham and D. K. Molzahn, "Error bounds on the DC power flow approximation: A convex relaxation approach," in *Proc. IEEE 55th Conf. Decis. Control (CDC)*, Dec. 2016, pp. 2411–2418.
[82] R. A. Jabr, "Radial distribution load flow using conic programming," *IEEE Trans. Power Syst.*, vol. 21, no. 3, pp. 1458–1459, Aug. 2006.
[83] R. A. Jabr, "Optimal power flow using an extended conic quadratic formulation," *IEEE Trans. Power Syst.*, vol. 23, no. 3, pp. 1000–1008, Aug. 2008, doi: 10.1109/TPWRS.2008.926439.
[84] X. Bai, H. Wei, K. Fujisawa, and Y. Wang, "Semidefinite programming for optimal power flow problems," *Elect. Power Energy Syst.*, vol. 30, no. 6, pp. 383–392, Dec. 2008.
[85] D. K. Molzahn, B. C. Lesieutre, and C. L. DeMarco, "Investigation of non-zero duality gap solutions to a semidefinite relaxation of the optimal power flow problem," in *Proc. 47th Hawaii Int. Conf. Syst. Sci.*, Jan. 2014, pp. 2325–2334.
[86] J. Lavaei and S. H. Low, "Zero duality gap in optimal power flow problem," *IEEE Trans. Power Syst.*, vol. 27, no. 1, pp. 92–107, Feb. 2012.
[87] C. Coffrin, H. L. Hijazi, and P. Van Hentenryck, "The QC relaxation: A theoretical and computational study on optimal power flow," *IEEE Trans. Power Syst.*, vol. 31, no. 4, pp. 3008–3018, Jul. 2016.
[88] S. Sojoudi and J. Lavaei, "Network topologies guaranteeing zero duality gap for optimal power flow problem," Dept. Ind. Eng. Oper. Res., Univ. California Berkeley, Berkeley, CA, USA, Tech. Rep., 2011.
[89] R. Madani, S. Sojoudi, and J. Lavaei, "Convex relaxation for optimal power flow problem: Mesh networks," *IEEE Trans. Power Syst.*, vol. 30, no. 1, pp. 199–211, May 2015.
[90] S. H. Low, "Convex relaxation of optimal power flow—Part I: Formulations and equivalence," *IEEE Trans. Control Netw. Syst.*, vol. 1, no. 2, pp. 15–27, Mar. 2014.
[91] R. P. O'neill, A. Castillo, and M. B. Cain, "The computational testing of AC optimal power flow using the current voltage formulations," Federal Energy Regulatory Commission, Washington, DC, USA, Tech. Rep., Dec. 2012.
[92] J. F. Franco, M. J. Rider, and R. Romero, "A mixed-integer linear programming model for the electric vehicle charging coordination problem in unbalanced electrical distribution systems," *IEEE Trans. Smart Grid*, vol. 6, no. 5, pp. 2200–2210, Sep. 2015.
[93] Z. Jiang, F. Li, W. Qiao, H. Sun, H. Wan, J. Wang, Y. Xia, Z. Xu, and P. Zhang, "A vision of smart transmission grids," in *Proc. IEEE Power Energy Soc. Gen. Meeting*, Jul. 2009, pp. 1–10, doi: 10.1109/PES.2009.5275431.
[94] H. Saadat, *Power System Analysis*, vol. 2. New York, NY, USA: McGraw-Hill, 1999.
[95] A. Gómez-Expósito, A. J. Conejo, and C. Ca nizares, *Electric Energy Systems: Analysis Operation*. Boca Raton, FL, USA: CRC Press, 2018.
[96] B. Cui and X. A. Sun, "A new voltage stability-constrained optimal power-flow model: Sufficient condition, SOCP representation, and relaxation," *IEEE Trans. Power Syst.*, vol. 33, no. 5, pp. 5092–5102, Sep. 2018.
[97] S. Kim, T. Song, M. Jeong, B. Lee, Y. Moon, J. Namkung, and G. Jang, "Development of voltage stability constrained optimal power flow (VSCOPF)," in *Proc. Power Eng. Soc. Summer Meeting. Conf. Process.*, vol. 3, Oct. 2001, pp. 1664–1669.
[98] Q. Wang and X. Sun, "The international journal of production research in the past, the present and the future: A bibliometric analysis," *Int. J. Prod. Res.*, vol. 57, nos. 15–16, pp. 4676–4691, Aug. 2019.
[99] R. J. Avalos, C. A. Canizares, and M. F. Anjos, "A practical voltage-stability-constrained optimal power flow," in *Proc. IEEE Power Energy Soc. Gen. Meeting-Convers. Del. Electr. Energy*, Feb. 2008, pp. 1–6.
[100] S. Boyd and L. Vandenberghe, *Numerical Optimization*. Cambridge, U.K.: Cambridge Univ. Press, 2004.
[101] J. Nocedal and S. J. Wright, *Numerical Optimization*. Berlin, Germany: Springer, 2006.
[102] L. K. Kirchmayer, *Economic Operation Power System*. New York, NY, USA: Wiley, 1958.
[103] G. Golub and C. Van Loan, *Matrix Computations*. Baltimore, MD, USA: Johns Hopkins University Press, 1996.
[104] D. R. Biggar and M. R. Hesamzadeh, *The Economics of Electricity Markets*. Hoboken, NJ, USA: Wiley, 2014.
[105] J. M. Morales, A. J. Conejo, H. Madsen, P. Pinson, and M. Zugno, *Integrating Renewables in Electricity Markets: Operational Problems*, vol. 205. Berlin, Germany: Springer, 2013.
[106] J. Momoh and L. Mili, *Economic Market Design and Planning for Electric Power Systems*, vol. 52. Hoboken, NJ, USA: Wiley, 2009.
[107] M. Shahidehpour and Z. Li, *Elecitricity Market Economics*. New York, NY, USA: Wiley, 2005.
[108] S. Chapman, *Electric Machinery Fundamentals*. New York, NY, USA: McGraw-Hill, 2005.
[109] A. J. Wood, B. F. Wollenberg, and G. B. Sheblé, *Power Generation, Operation, and Control*. Hoboken, NJ, USA: Wiley, 2013.
[110] F. A. Potra and S. J. Wright, "Interior-point methods," *J. Comput. Appl. Math.*, vol. 124, nos. 1–2, pp. 281–302, Jan. 2000.
[111] Anonymous. (2021). *Newton's Method*. [Online]. Available: https://en.citizendium.org/wiki/Newton's_method
[112] T. J. Ypma, "Historical development of the Newton–Raphson method," *SIAM Rev.*, vol. 37, no. 4, pp. 531–551, 1995.
[113] A. Gomez-Exposito, A. J. Conejo, and C. Canizares, *Electric Energy Systems: Analysis and Operation*. Boca Raton, FL, USA: CRC Press, 2008.
[114] J. L. Kirtley, *Electric Power Principles: Sources, Conversion, Distribution Use*. Hoboken, NJ, USA: Wiley, 2011.
[115] D. Karnopp, D. L. Margolis, and R. C. Rosenberg, *System Dynamics: A Unified Approach*, 2nd ed. New York, NY, USA: Wiley, 1990. [Online]. Available: http://www.loc.gov/catdir/enhancements/fy0650/90012110-t.html
[116] F. T. Brown, *Engineering System Dynamics*, 2nd ed. Boca Raton, FL: CRC Press, 2007.
[117] P. Palensky and D. Dietrich, "Demand side management: Demand response, intelligent energy systems, and smart loads," *IEEE Trans. Ind. Informat.*, vol. 7, no. 3, pp. 381–388, Aug. 2011.

AMRO M. FARID (Senior Member, IEEE) received the B.Sc. degree, in 2000, the M.Sc. degree in mechanical engineering from MIT, in 2002, and the Ph.D. degree in engineering from the University of Cambridge, U.K. He is currently a Visiting Associate Professor of Mechanical Engineering at MIT and an Associate Professor in Engineering at the Thayer School of Engineering, Dartmouth College. He leads the Laboratory for Intelligent Integrated Networks of Engineering Systems (LIINES) and has authored over 150 peer-reviewed publications in smart power grids, energy-water nexus, electrified transportation systems, industrial energy management, and interdependent smart city infrastructures. He holds leadership positions in the IEEE Smart Cities Program, Control Systems Society (CSS), the Power & Energy Society (PES), and the Systems, Man & Cybernetics Society (SMCS).